

# Mechanochemistry: One Bond at a Time

Jian Liang and Julio M. Fernández\*

Department of Biological Sciences, Columbia University, New York, New York 10027

**ABSTRACT** Single-molecule force-clamp spectroscopy offers a novel platform for mechanically denaturing proteins by applying a constant force to a polyprotein. A powerful emerging application of the technique is that, by introducing a disulfide bond in each protein module, the chemical kinetics of disulfide bond cleavage under different stretching forces can be probed at the single-bond level. Even at forces much lower than that which can rupture the chemical bond, the breaking of the S—S bond at the presence of various chemical reducing agents is significantly accelerated. Our previous work demonstrated that the rate of thiol/disulfide exchange reaction is force-dependent and well-described by an Arrhenius term of the form  $r = A(\exp((F\Delta x_r - E_a)/k_B T))$  [nucleophile]. From Arrhenius fits to the force dependency of the reduction rate, we measured the bond elongation parameter,  $\Delta x_r$ , along the reaction coordinate to the transition state of the  $S_N2$  reaction cleaved by different nucleophiles and enzymes, never before observed by any other technique. For S—S cleavage by various reducing agents, obtaining the  $\Delta x_r$  value can help depicting the energy landscapes and elucidating the mechanisms of the reactions at the single-molecule level. Small nucleophiles, such as 1,4-DL-dithiothreitol (DTT), tris(2-carboxyethyl)phosphine (TCEP), and L-cysteine, react with the S—S bond with monotonically increasing rates under the applied force, while thioredoxin enzymes exhibit both stretching-favored and -resistant reaction-rate regimes. These measurements demonstrate the power of the single-molecule force-clamp spectroscopy approach in providing unprecedented access to chemical reactions.

**KEYWORDS:** single-molecule force spectroscopy · atomic force microscopy (AFM) · disulfide bond · protein · force-clamp spectroscopy · thioredoxin · bimolecular nucleophilic substitution ( $S_N2$ )

Force is one of the most common variables and concepts in physics which has been studied for thousands of years. It plays crucial roles in almost everything from the motion of stars in the universe to the organization of atoms into structured matters. In chemistry, whose main concern is investigating the rules of nature at atomic and molecular level, especially those related to the formation and breaking of chemical bonds, force is also a ubiquitous and key factor. For instance, grinding of solids by pestles in mortars, chewing of food, and scissoring of a piece of paper all involve force-induced chemical bond cleavage. There have been many reports in the literature bridging force and chemical reactions, such as reactions under

mechanical pressures,<sup>1,2</sup> bond strains in molecules,<sup>3,4</sup> and spectroscopic studies of interatomic forces within molecules.<sup>5</sup> In the last case, a classical example is that by measuring the vibrational frequency of the stretching mode of a specific chemical bond and assuming the bond is a harmonic spring connecting the two atoms the force constant of the bond can be derived.<sup>6</sup> In this scenario, a chemical bond can cleave if being stretched by large enough pulling forces from both ends. Many studies of mechanochemistry have been carried out by stretching or compressing macroscopic pieces of polymers or other materials and recording observable changes in their properties.<sup>7,8</sup> However, when it comes to the molecular level, surprisingly little is known about the effect of mechanical forces on the reactivity of a single bond.

Over the past 15 years, a number of experimental techniques have been developed to make possible understanding the role of mechanical force on biological and chemical systems at single-molecule level, including optical tweezers, magnetic tweezers, and atomic force microscopy (AFM).<sup>9–16</sup> In optical tweezers,<sup>13,14</sup> a focused laser beam exerts radiation pressure on a micrometer-sized dielectric bead, which experiences a force proportional to the gradient of the laser intensity. The molecule of interest (frequently a micrometer-scale DNA molecule) is attached to the bead through a noncovalent bond (e.g., biotin—avidin). The other end of the molecule is attached either to a coverslide surface or to a second bead, where this second bead is either held in another optical trap or fixed by suction on a micropipet. The force applied to the molecule can be controlled by modulating the laser trapping on

\*Address correspondence to jfernandez@columbia.edu.

Published online July 2, 2009.  
10.1021/nn900294n CCC: \$40.75

© 2009 American Chemical Society

one of the beads, moving the surface using a piezoelectric positioner or moving the suction micropipet. In magnetic tweezers,<sup>15,16</sup> a DNA molecule is noncovalently attached between a magnetic bead and a glass coverslide. Two or more magnets are positioned over the coverslide, and the force applied to the bead (and thus, the DNA molecule) is proportional to the gradient of the magnetic field at the position of the bead. In AFM,<sup>17–21</sup> the molecule is held between a sharp tip mounted at the end of a cantilever and the substrate on a piezoelectric stage. The stage extends or retracts along the axial direction, exerting force through the molecule to the cantilever. Displacement of the cantilever is measured from the deflection of a laser beam from the backside of the cantilever into a position-sensitive detector. The force on the molecule can be calculated from the spring constant and the displacement of the cantilever, and the extension of the molecule is equal to the separation between the tip and the sample surface. In general, each of these three techniques has its own features and limitations and should be selected carefully in different single-molecule spectroscopic applications. However, regardless of the specific detection method, single-molecule events should be identified by clear and unambiguous fingerprints, which usually are difficult to obtain and can easily be buried in the background noise.

The first biological polymer characterized by force spectroscopy at single-molecule level was double-stranded DNA stretched with magnetic tweezers.<sup>22</sup> A few years later, the mechanical unfolding of a single polyprotein was reported using both AFM and optical tweezers.<sup>23,24</sup> Since then, AFM-based single-molecule force spectroscopy has achieved great success in single-molecule imaging and manipulation,<sup>25–28</sup> especially in the study of mechanical design and folding properties of proteins.<sup>29–33</sup> More recently, chemical reactions at single-molecule level were probed using this technique.<sup>34–36</sup> In this type of experiment, how to anchor the target single molecule between the substrate and the AFM tip is not trivial. Both experimental and theoretical investigations suggest the pulling force necessary to break a chemical bond be a few nanonewtons,<sup>1,37–39</sup> while rupturing structures maintained by noncovalent bonds, such as unfolding of proteins, overcoming protein–ligand interactions, and unraveling a single base-pair in double-stranded DNAs requires forces at least 1 order of magnitude smaller.<sup>40–43</sup> A few reports<sup>37,38</sup> have been published on bonding the molecule covalently at both ends before the pulling experiments, while in the majority of experiments, the molecule is picked up randomly through nonspecific interactions. Consequently, the adhesion between the AFM tip and the molecule, or between the molecule and the substrate surface, is weak compared with the force required to break a chemical bond but probably comparable to the hydrogen bonds and hy-

drophobic interactions maintaining the secondary and tertiary structure of a protein (without disulfide bonds). Before reaching the force threshold to cleave a chemical bond, the molecule would very likely have detached from the cantilever or from the substrate since the weakest linkage always has the highest probability of breaking. This is probably the major reason that it has been a rather common practice of pulling a globule protein into a peptide chain while experimental examples of directly breaking a chemical bond by stretching force are much fewer. Under forces much lower than bonding interactions, we can, however, still observe chemical reactions being remarkably accelerated.<sup>36</sup> In this case, force speeds up the reaction rate by doing mechanical work or “injecting” energy into the reactants and helping them cross the activation energy barrier, in the direction of the reaction coordinate since all chemical reactions involve bond elongation until the final bond cleavage.

In single-molecule spectroscopic experiments conducted by AFM, there are two popular types of operational modes: force-extension (constant-velocity) mode and force-clamp (constant-force) mode (Figure 1). In force-extension mode,<sup>45–48</sup> the piezoelectric stage is moved away from the cantilever at a constant velocity, and the force applied to the molecule is recorded as a function of time or molecular extension. As the distance between the tip and substrate increases, the force applied to the single molecule tethered between the two ends also increases with time until an event (unfolding of a protein or breaking of a chemical bond) occurs, resulting in a peak in the force-extension recording. Immediately after the event, the force drops rapidly but then begins to increase again until the next event. This process can be repeated many times, resulting in a sawtooth pattern (Figure 1B), until the molecule detaches from the tip or from the surface. The sawtooth pattern exhibits a reproducible characteristic shape that can usually be fit with the worm-like chain (WLC)<sup>49,50</sup> or freely jointed chain (FJC)<sup>22</sup> model of polymer elasticity. Numerous information, including the contour length of the molecule before and after each event and the force required to trigger the event, can then be obtained, which offers the fingerprints for distinguishing single-molecule signals from possible spurious background

**VOCABULARY: single-molecule force spectroscopy** – experiments where single molecules are mechanically stretched and their elastic response is recorded in real time • **atomic force microscopy (AFM)** – one of the scanning probe microscopy techniques for imaging, measuring, and manipulating matter at the nano- or molecular scale; a mechanical cantilever probes the force interaction with the surface and creates a feedback signal for the piezoelectric elements that respond with tiny but accurate movements to complete the scanning • **force-clamp spectroscopy** – one of the AFM-based single-molecule force spectroscopy techniques that operates at constant-force mode; the feedback system adjusts the length of the molecule being stretched such that the deflection of the cantilever remains at the set point • **bimolecular nucleophilic substitution (S<sub>N</sub>2)** – a type of nucleophilic substitution, where a lone pair of electrons on a nucleophile attacks an electron-deficient center and forms a new chemical bond, expelling and replacing the leaving group

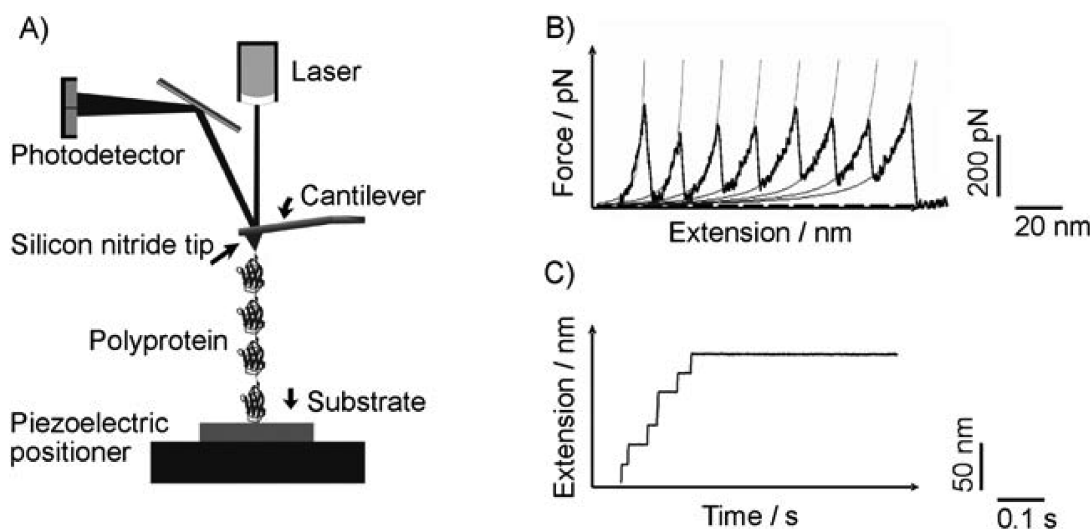
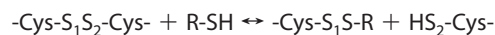


Figure 1. (A) Simplified diagram of the AFM in a single-molecule force experiment. (B) When a polyprotein is pulled at constant velocity (force-extension mode), the increasing pulling force triggers the unfolding of a module. Continued pulling repeats the cycle, resulting in a force-extension curve with a characteristic “sawtooth pattern”. (C) When pulling is done under feedback, the piezoelectric actuator adjusts the extension of the polyprotein to keep the pulling force at a constant value (force-clamp mode). Unfolding now results in a staircase-like elongation of the protein as a function of time. Reproduced from ref 44. Copyright 2008 Wiley-VCH Verlag GmbH & Co. KGaA.

noises. In force-extension recordings, the force is not a constant value but evolves over time. For better assessing the effect of a given force on a process of interest, the second operational mode, so-called force-clamp (constant-force) AFM,<sup>51–55</sup> offers the opportunity of controlling the force as an independent variable. In force-clamp spectroscopy, the extension of the molecule is recorded as a function of time, while the force is held constant or in more complex forms, such as rectangular or triangular pulses. When an unfolding or bond-breaking event occurs, a stepwise increase would appear in the recorded trace, and repeating of these events would shape the final recording into a staircase form (Figure 1C).

Our group has been working on AFM-based single-molecule force spectroscopy in the past 10 years.<sup>56</sup> In this review, we mainly discuss the single-molecule force-clamp spectroscopy approach we employed recently on the chemical cleavage of disulfide (S–S) bonds, through bimolecular nucleophilic substitution ( $S_N2$ ) reactions, while related works carried out by other researchers would also be included. A recent survey<sup>57</sup> in the Protein Data Bank (PDB) identified 42 960 unique disulfide bonds in 31 611 protein structures solved by X-ray crystallography, indicating the commonality of disulfides in protein design. These disulfide bonds, known to be the strongest interaction in protein’s tertiary structures, play a variety of roles,<sup>58,59</sup> including control of the kinetics of protein folding or the population of intermediate states and the thermodynamic and mechanical stabilization of proteins in their native states. Interestingly, the introduction of disulfide bonds by protein engineering can be used to selectively “lock” proteins into particular conformations.<sup>60</sup>

Disulfide formation in proteins typically involves a pair of cysteines, and the disulfide bond reduction usually occurs through the thiol/disulfide exchange reaction:



In this typical  $S_N2$  reaction, RSH performs the nucleophilic attack using the electron lone pair on its sulfur atom on one of the sulfur atoms in the disulfide bond ( $S_1$ ), propelling  $-\text{Cys-S}_2\text{H}$  as the leaving group. It is worth noting that sulfur is not the only atom that can complete the  $S_N2$  reaction. Actually, phosphorus-based compounds, such as tris(2-carboxyethyl)phosphine (TCEP), have been widely used as reducing agents to cleave disulfide bonds in proteins.<sup>61,62</sup> Dynamic cycles of disulfide bond reduction and oxidation play key roles in the function of a number of proteins.<sup>63,64</sup> Especially, many native proteins contain disulfide bonds that are exposed to mechanical forces *in vivo*. Some examples include cellular adhesion proteins such as cadherins,<sup>65</sup> selectins,<sup>66</sup> and IgCAMs.<sup>67</sup> Others are important in maintaining the extracellular matrix, such as fibronectin,<sup>68</sup> or in tissue elasticity, such as fibrillin<sup>69</sup> and titin.<sup>70</sup> The regulation of the redox state of disulfide bonds by mechanical stress indicates that force can be converted into biochemical signals,<sup>71,72</sup> and the intertwining between chemistry and mechanics can be ubiquitous in biological phenomena. Therefore, a complete understanding of the dynamics of disulfide bond reactions in proteins, particularly under applied forces, is important for biology and chemistry studies. Furthermore, our experimental approach is not limited to, although has been focused on, cleavage of disulfide bonds and can be expanded

to understanding the mechanochemistry of other chemical reactions.

In the following sections, we will first present details about the protocols of our experimental design, including the molecular biology method for the preparation of polyproteins, technical specifications of our AFM, and the data analysis processes. Second, we address the results of applying a constant stretching force to the engineered disulfide bonds and measuring the rate of reduction initiated by small nucleophiles. We find that the reduction rate is linearly dependent on the concentration of the nucleophile and is exponentially dependent on the applied force ( $F$ ), which is well-described by an Arrhenius term of the form<sup>73–75</sup>

$$r = A(\exp((F\Delta x_r - E_a)/k_B T)[\text{nucleophile}]) \quad (1)$$

where  $A$  is the pre-exponential factor,  $E_a$  is the activation energy barrier,  $k_B$  is Boltzmann's constant,  $T$  is the temperature, and  $\Delta x_r$  is the distance to the transition state along the reaction coordinate. From the force dependency of the reduction rate, we can measure  $\Delta x_r$  ( $\sim 0.2\text{--}0.5$  Å), which is related to the bond elongation up to the transition state of the  $S_N2$  reaction, never before observed by other techniques. Third, we discuss thioredoxin-catalyzed disulfide bond cleavage under stretching forces, which is of special interest when comparing the reactivity of enzymes from different species. Last but not least, some examples of the conversion of mechanically induced chemical reactions into actual biological functions will be presented. In general, our work reveals that the kinetics of chemical reactions accompanied by bond elongation is force-dependent, and AFM-based force-clamp spectroscopy offers a powerful tool to access chemical reactions with unprecedented details at the single-bond level.

**Experimental Design. Construction of Poly(I27) Proteins and Engineering of the Disulfide Bond.** In early force spectroscopy experiments on polyproteins with natural disulfide bridges,<sup>76,77</sup> both the total number of amino acids and the position of the disulfide bond are different in each protein domain, resulting in broad statistical distributions of the forces and the elongations in the force spectra. Therefore, the design of a multimodular protein with well-defined identical structures is an important prerequisite for reducing the complexity in the interpretation of the experimental data. The protein we have been using to probe disulfide bond reactions with single-molecule force-clamp spectroscopy is composed of direct tandem repeats of Ig module 27 of the I band

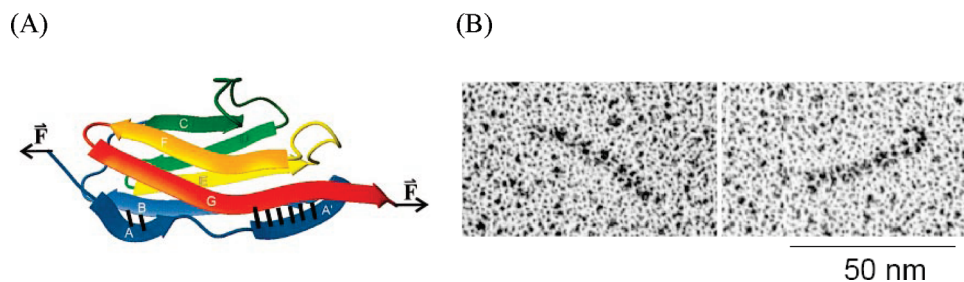


**Figure 2.** (A) Three-dimensional structure of I27 (from SCOP database) and schematic illustration of the pulling directions, showing the “shear pattern” model for the H-bond breakage in the I27 domain, where the critical H bonds (black lines) break simultaneously. Seven  $\beta$ -strands (each of them shown as a ribbon arrow of a different color) are folded into two  $\beta$ -sheets, one comprising strands A, B, D, E and the other including strands A', C, F, G. Reproduced from ref 21. Copyright 2000 Elsevier B.V. (B) Electron microscopy images of rod-like  $(I27)_{12}$  polyproteins (courtesy of Dr H. P. Erickson). Reproduced from ref 78. Copyright 1999 Elsevier B.V.

of human cardiac titin (I27). Titin I27, an 89-residue  $\beta$ -sandwich protein (Figure 2), is the first structurally determined Ig domain from the I-band region responsible for regulating passive elasticity of muscle sarcomere,<sup>53,79</sup> and therefore, its mechanically induced reversible folding and unfolding properties have attracted massive interest. The extension of I27 under an applied force has also been rigorously modeled using steered molecular dynamics simulations.<sup>80–83</sup> The preparation of the polyprotein has been described in detail in our previous work.<sup>21,84</sup> The number of protein modules in the polyprotein can be controlled, and the most frequently used one contains eight identical repeats of I27, noted as  $(I27)_8$ . It is worth noting that polyproteins composed of repeats of other modules, such as ubiquitin, can also be prepared in a similar manner,<sup>85,86</sup> although they have not been utilized in the study of disulfide bond reductions.

In folded I27, two sets of interstrand hydrogen bonds firmly lock the terminal regions to prevent spontaneous unraveling, as shown in Figure 2. Through cysteine mutagenesis,<sup>36</sup> we engineer a disulfide bond in the I27 domain between the 32nd and 75th residues (named  $I27_{G32C-A75C}$ ) by mutating the 32nd glycine (G) and 75th alanine (A) to two cysteines (C), which are closely positioned in space as determined by the NMR structure of wild-type I27 (PDB ID code 1TIT). The disulfide bridge is buried in the folded state of the protein and not accessible to solvent or the reducing agent. Native Cys-47 and Cys-63, which do not form a disulfide bond, are mutated to alanines to avoid unwanted polymerizations. We prepare an eight-domain N–C covalently linked polyprotein of this  $I27_{G32C-A75C}$  through rounds of successive cloning, followed by expression of the gene in *Escherichia coli* (*E. coli*) as described in ref 21. Pelleted cells are lysed by sonication, and the protein is purified first by immobilized metal ion affinity chromatography (IMAC) and then by gel filtration. The protein is stored at 4 °C in HEPES or phosphate buffered saline (PBS) buffer (pH 7.2). Other polyproteins with the disulfide bond at different positions, such as

(I27<sub>E24C-K55C</sub>)<sub>8</sub> and (I27<sub>P28C-K54C</sub>)<sub>8</sub>, can be constructed following similar procedures.

**Single-Molecule Force-Clamp Spectroscopy.** Typically, our custom-built atomic force microscope is equipped with a modified Digital Instruments (Veeco Instruments, Santa Barbara, CA) detector head (AFM-689) and a PicoCube P363.3-CD piezoelectric translator (Physik Instrumente, Karlsruhe, Germany) controlled by an analog proportional-integral-differential (PID) feedback system.<sup>85</sup> The PID amplifier is driven by an error amplifier that compares a force set point with the actual force measured. The actuator has a displacement range of 6500 nm in the z axis, with a bandwidth limited by an unloaded resonant frequency of  $\sim 10$  kHz, which is somewhat reduced by an aluminum pedestal where the gold-coated coverslide is placed. Subnanometer resolution results from a fast capacitive sensing of the actuator's position, with peak-to-peak noise of  $\sim 0.5$  nm. The cantilever we use is the Veeco MLCT silicon nitride probe with a typical spring constant of  $\sim 15$  pN/nm, which is calibrated as previously reported.<sup>52</sup> It is not rare to find cantilevers where the overall drift in the system (unfolded protein plus cantilever plus piezoelectric actuator) is  $< 1$  nm over 10 s or more. Under force-clamp conditions, the force signal has a standard deviation that is bandwidth-dependent. A force signal filtered at  $\sim 150$  Hz typically has a standard deviation of  $\sim 2.5$  pN. Our force-clamp apparatus is able to complete a force step in less than 10 ms. The applied force can be a step which is used to stretch proteins at a constant force or a ramp which is used to stretch proteins at a force that increases (or decreases) linearly with time.

All experiments are conducted at room temperature ( $\sim 298$  K) in PBS or HEPES buffer with the indicated amount of reducing agent. Buffers are controlled to pH 7.2 unless otherwise specified. Small changes in active reducing agent concentration due to evaporation and air oxidation do not have great effect on our results, and the traces compiled over a whole day demonstrate similar reaction kinetics. A few microliters of protein sample are applied in each experiment, which is only  $\sim 1\%$  the total volume of the solution, causing negligible change to the concentration of the reducing agent. Gold-coated coverslides are used because they result in a better pick-up rate than glass coverslides even in the absence of thiolate-gold bonds. A droplet of protein solution is first pipetted onto the coverslide, and then an O-ring-sealed liquid cell is placed on top of it. Solution containing the reducing agent is injected into the liquid cell through a syringe and mixed with the protein sample. Single protein molecules are stretched by first pressing the cantilever on the coverslide for  $\sim 2-3$  s at 350–800 pN, then retracting at a constant force. Our success rate at picking up a single molecule is  $\sim 1\%$  of all the trials. In a typical experiment, the molecule is first stretched for  $< 1$  s at 130–180 pN to unfold the protein modules and to expose the disul-

fide bonds, and then for a time period depending on the reaction rate at the second force pulse.

**Data Analysis.** All data are obtained and analyzed using custom software written in IGOR Pro (WaveMetrics, Lake Oswego, OR), as recordings of the extension of the molecule versus time. The first set of fingerprints of (I27<sub>G32C-A75C</sub>)<sub>8</sub> in the force spectroscopy is a series of well-resolved steps of  $\sim 10-11$  nm during the first force pulse. This number slightly varies depending on the force because of the elasticity of the extended polypeptide. The first force pulse unfolds each protein module up to the mechanical clamp formed by the disulfide bond, exposing the disulfide bond to the solvent and the reducing agent. This step height is significantly lower than that ( $\sim 24$  nm) expected for native I27 (without the engineered disulfide bond) unfolding.<sup>87</sup> This shortening actually indicates the formation of the engineered disulfide bond within the protein module. The unfolding of 46 "unsequestered" residues (1–31 and 76–89) has a predicted step size of 10.4 nm, which can be measured from the force-extension curve of the protein.<sup>36</sup> This value is very similar to the step height, indicating that, after the first force pulse, the disulfide bond in each module is directly under the applied stretching force, forming a covalent barrier "trapping" residues 33–74 and preventing complete unfolding of each module. The force for this stage is usually between 100 and 200 pN and lasts less than 1 s because of the relatively fast kinetics of unfolding of the protein and the necessity to avoid the disulfide bond reduction at this stage. If the bond were to be ruptured by force alone, we would expect to observe a second step corresponding to the extension of the trapped polypeptide. We do not, however, observe any such steps without the presence of reducing agents. This outcome is in agreement with previous discussions, where forces  $< 1$  nN cannot break a covalent bond. The second set of fingerprint steps is observed in the following second force pulse, with the presence of nucleophile, where the chemical reaction on the disulfide bond happens. The height of this set of steps is  $\sim 14$  nm, which is again in good agreement with the value obtained from force-extension experiments. These two types of steps should be carefully distinguished by their heights, and traces that have mixed unsequestered unfolding and reduction events during the second force pulse should not be allowed to enter the subsequent statistical analysis. The timing of the kinetics of disulfide bond reduction events starts at the beginning of the second pulse. The reduction rate is adjusted by controlling the concentration of the reducing agent, so that the measured rate falls in the capable range of our instrument ( $\sim 0.05$  to  $\sim 15$  s<sup>-1</sup>). The lower limit comes from the required long pulling time at slow rate (see discussions below) during which the accumulated drift becomes significant. The upper limit comes, however, from the relaxation of pulling force when the reduction events happen. Al-

though the feedback system quickly restores the force in  $\sim 10$  ms or shorter, the total relaxation time, during which the force is deviated from the set point value, may not be negligible when the rate is fast. In this two-stage protocol, the mechanical unfolding of the protein in the first stage is, in the majority of acquired traces, kinetically separated from disulfide bond reduction in the second stage, making it possible to directly study force-dependent disulfide bond reduction.

We assume that disulfide reduction in our protein is Markovian (*i.e.*, each reduction event is independent of all others); thus, summing up and then normalizing traces with reduction steps (stages IV and V in Figure 3) will result in invariant exponential kinetics.<sup>85</sup> By fitting the summed and normalized traces with the following single-exponential function of time, the disulfide reduction rate can be derived

$$P_r(t) = 1 - \exp\left(-\frac{t}{\tau_r}\right) \quad (2)$$

where  $P_r(t)$  is the probability of completion of a reduction event, and  $\tau_r$  is the time constant of the exponential increase. The reaction rate, given by  $r = 1/\tau_r$ , measures the number of reduction events happening per unit time. Here, the rate is not the actual time each bond takes to cleave, which might be as short as picoseconds and far exceeds the time resolution of our AFM. It is important to point out that the second force pulse should last long enough to allow all the disulfide bond reactions to happen. Failure to do so may result in overestimate of the reaction rate. As can be calculated from eq 2,  $P_r(t) = 0.865, 0.950, 0.982,$  and  $0.993,$  respectively, when  $t = 2\tau_r, 3\tau_r, 4\tau_r,$  and  $5\tau_r.$  The probability of reactions happening to all eight independent S–S bonds is  $[P_r(t)]^8$  and therefore equals 31, 66, 86, and 95%, correspondingly. Hence, it is necessary for the cantilever to hold the polyprotein at the second force pulse for a time period at least  $\sim 4\text{--}5$  times the  $\tau_r.$  Last but not least, the error bars of the data points are obtained by bootstrapping. In this method, the entire set of traces (typically containing  $\sim 20$  traces or more, one of which is shown in Figure 3) is partitioned into random subsets. The traces in each subset are then averaged and fit with the same single exponential (eq 2) to obtain the reaction rate for the subset. The average value and the standard deviation of the rate for the whole set are then statistically calculated from the rates of all the subsets. This standard deviation is used as the magnitude of the error bars shown in the figures.

**Disulfide Bond Reduction Reactions by Small Nucleophiles. The First Investigation: Disulfide Bond Reduction by DTT.** The first chemical reaction we studied using our single-molecule

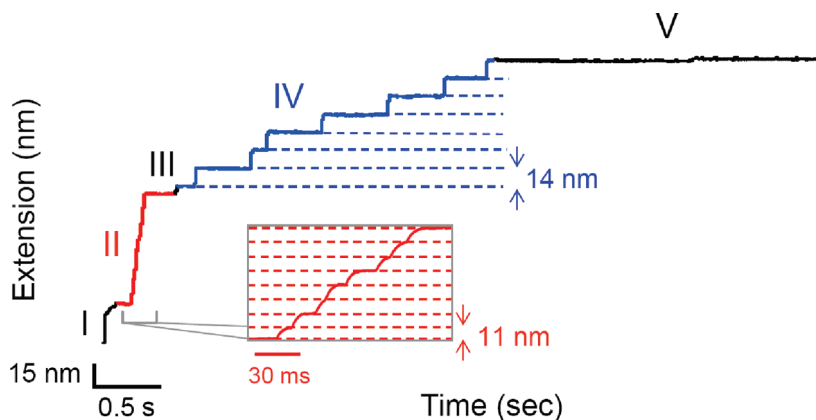
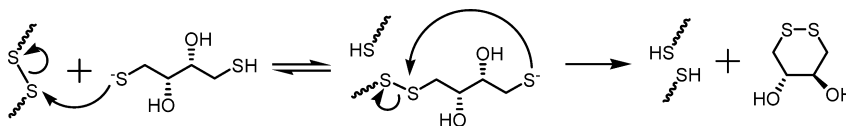


**Figure 3.** A typical trace of single-molecule force-clamp spectroscopy, marked as different stages during pulling in different colors to guide the eyes. I (black): As the substrate is withdrawn, the polyprotein is elastically elongated and other bonds between the tip and the substrate are disconnected,<sup>88</sup> causing the initial extension until a single protein forms the only connection between the two surfaces. II (red): A quick increment of extension containing a series of  $\sim 11$  nm steps (inset), indicating the unfolding of the domains of the polyprotein. III (black): Because of different force intensities of the two force pulses, a further elastic extension or contraction appears when the second force pulse begins to apply. IV (blue): The second set of steps, with  $\sim 14$  nm height, fingerprints the disulfide bond reduction events. V (black): All of the events have happened, and the trace shows no more extension.

technique is between 1,4-DL-dithiothreitol (DTT) and the disulfide bond. DTT is a dithiol reducing agent which has been widely used in preventing disulfide bond formations between thiolated DNAs or between cysteine residues in proteins.<sup>89,90</sup> The typical reduction of a disulfide bond by DTT proceeds through two sequential thiol/disulfide exchange reactions, which are illustrated in Scheme 1, forming oxidized DTT and leaving behind a reduced disulfide bond. In this reaction scheme, the first step causes the cleavage of the S–S bridge in the protein and correspondingly an increment of extension is detected in our single-molecule force spectroscopy. The equilibrium of this step is driven far to the right because the two sulfur atoms in the initial disulfide bond are mechanically separated after the cleavage (Figure 4A). The second thiol/disulfide exchange reaction, in which DTT forms a highly stable six-member ring with an internal disulfide bond and leaves the polypeptide chain, is not detected. As demonstrated in Figure 4, stretching the  $(I27_{G32C-A75C})_8$  polyprotein under force-clamp conditions using the two-pulse protocol results in unsequestered unfolding, and subsequently, the thiol/disulfide exchange can occur if DTT is present in solution. Unfolding the protein is a prerequisite for the chemical reaction because previous studies indicated that the disulfide bond in  $I27_{G32C-A75C}$  is particularly solvent-inaccessible in the folded state.<sup>91</sup> After this first series of  $\sim 11$  nm steps relating to protein unfolding and only in the presence of



**Scheme 1.** Reaction between DTT and a disulfide bond.

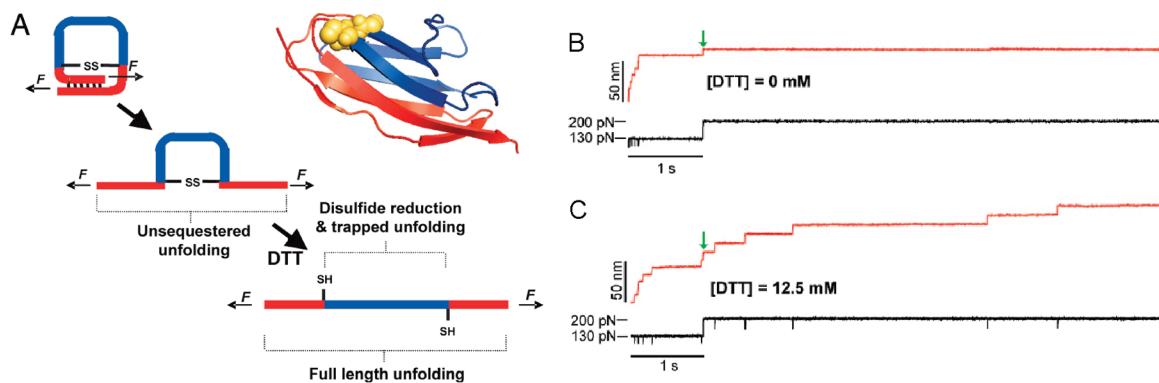


Figure 4. (A) In the ribbon structure of I27<sub>G32C-A75C</sub>, mutated residues 32 and 75 are shown as yellow spheres, while residues 1–31 and 76–89 are pictured in red (unsequestered residues), and 33–74, behind the disulfide bond, are in blue (trapped residues). The cartoons on the left depict the three sequential events that take place when we apply a mechanical force to the I27<sub>G32C-A75C</sub> protein, as discussed in the main text. (B) Typical double-pulse force-clamp experiment pulling the (I27<sub>G32C-A75C</sub>)<sub>8</sub> protein first at 130 pN for 1 s and then stepping to a force of 200 pN (black trace). The first pulse causes unsequestered unfolding events (~11 nm steps). Upon increasing the force to 200 pN (green arrow), we observe an elastic step elongation of the protein. In the absence of DTT, no further steps are observed. (C) Repeating the same experiment in the presence of 12.5 mM DTT and after the elastic elongation of the protein (green arrow), we observe a series of five steps of ~14 nm corresponding to the disulfide reduction events. Reproduced from ref 36. Copyright 2006 National Academy of Sciences, U.S.A.

DTT (12.5 mM), a series of additional ~14 nm steps appear that mark single thiol–disulfide exchange reactions, whereas no further steps are observed in the absence of DTT. It is worth noting again that, upon switching to a new force value, an elastic extension (when the force increases) or contraction (when the force decreases) of the polyprotein would show in the spectrum and should not be mistaken as an unfolding or reduction event.

To measure the rate of reduction at a certain force, we repeat many times the pulse pattern shown in Figure 4, obtaining an ensemble of single-molecule recordings. Figure 5A shows three recordings achieved under the same conditions, demonstrating the stochastic nature of both the unsequestered unfolding and the thiol/disulfide exchange events. This stochastic nature decides that the reaction rate cannot be judged from a single trace. The average of the ensemble in Figure 5B

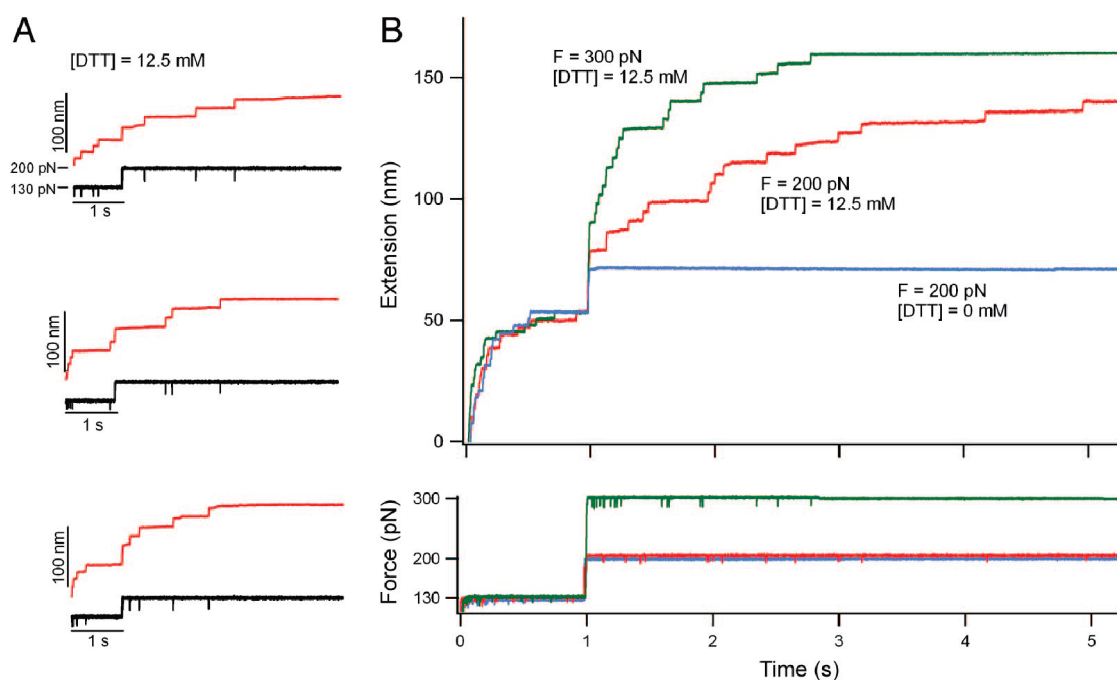
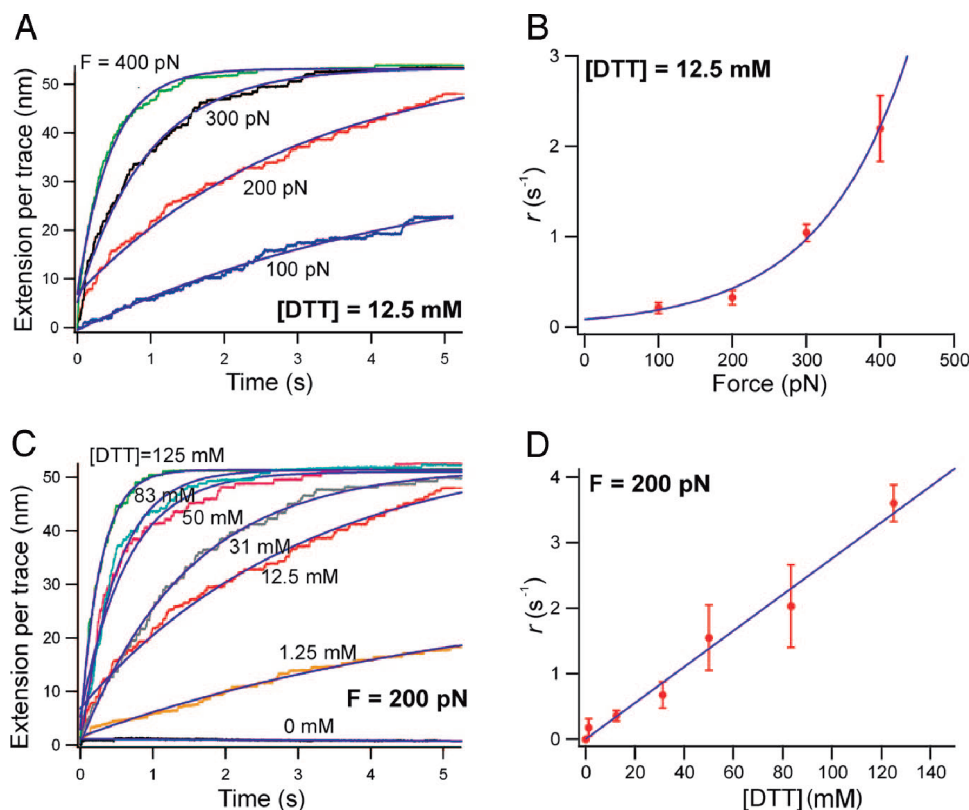


Figure 5. Ensemble measurements of the kinetics of thiol/disulfide exchange. (A) Three recordings are shown of single (I27<sub>G32C-A75C</sub>)<sub>8</sub> polyproteins that are extended with the same double-pulse protocol. The stochastic nature of both the unsequestered unfolding events as well as the thiol/disulfide exchange events becomes apparent when comparing these recordings. (B, top) Four-trace average (red trace) of the double-pulse experiments shown in (A) demonstrates the methods used to build up an ensemble of recordings. Similar four-trace averages are shown for data obtained under two other conditions: 12.5 mM DTT,  $F = 130$  pN for 1 s then  $F = 300$  pN (green trace); and 0 mM DTT,  $F = 130$  pN for 1 s then  $F = 200$  pN (blue trace). (B, bottom) Averaged force pulses. Reproduced from ref 36. Copyright 2006 National Academy of Sciences, U.S.A.

demonstrates that protein unfolding during the first pulse is independent of DTT, following a similar exponential time evolution at the same force. However, thiol/disulfide exchange during the second pulse appears both DTT- and force-dependent. Hence, in the subsequent analysis, we can ignore the unsequestered unfolding observed during the first pulse and only analyze the thiol/disulfide exchange events in the second pulse. Obviously, when more traces and events are gathered into the ensemble, the averaged (summed and normalized) trace would fit better the exponential function and the measured rate would be more precise. In our experiments, typically  $>20$  traces containing  $\sim 100$  events are collected for one data point of the reaction rate.

Figure 6A shows multiple ( $\sim 25$ ) trace averages of only the second pulse at different forces holding a constant DTT concentration. By fitting the single exponential to each of the averages, we obtain the rate of thiol/disulfide exchange as  $r = 1/\tau_r$  (eq 2). Figure 6B demonstrates that  $r$  is exponentially dependent on the applied force ranging from 100 to 400 pN. Similarly, Figure 6C,D shows the results of experiments conducted at different concentrations of DTT while holding the force constant. In this case,  $r$  has linear dependence on the concentration of DTT, consistent with the  $S_N2$  mechanism of the thiol/disulfide exchange reaction. Both the force and concentration dependencies are in accordance with the Arrhenius form (eq 1). Interestingly,  $r$  is independent of the number of protein modules in a single polyprotein, which is consistent with the memory-less Markovian behavior of each module<sup>85</sup> and with the fact that the measured unfolding rates of (Ubiquitin)<sub>9</sub> and (I27)<sub>8</sub> present a close agreement with those of their corresponding monomers [(Ubiquitin)<sub>1</sub> and (I27)<sub>1</sub>].<sup>87</sup> These results suggest that we can obtain the same exponential growth (after normalization) of extension as shown in Figure 6 using (I27<sub>G32C-A75C</sub>)<sub>1</sub> instead of (I27<sub>G32C-A75C</sub>)<sub>8</sub> if the same amount of reduction events are collected. Nevertheless, construction of tandem repeats in a polyprotein for force-clamp experiments has remarkable advantages. For instance, the data acquiring process is facili-



**Figure 6.** The thiol/disulfide exchange chemical reaction is force- and [DTT]-dependent. Only the second pulse averages are shown; time = 0 s denotes the start of the second pulse. (A) Sets of trace averages ( $n > 20$  in each set) measured at a constant concentration of DTT (12.5 mM), while varying the force of the second pulse between 100 and 400 pN. Single-exponential fits (continuous lines) measure the time constant,  $\tau_r$ , of the thiol/disulfide exchange. (B) Plot of the rate of the thiol/disulfide exchange,  $r = 1/\tau_r$ , as a function of the pulling force at [DTT] = 12.5 mM. The solid line is an exponential fit to the data. (C) Trace averages measured at a constant pulling force ( $F = 200$  pN) but at various DTT concentrations. (D) Plot of  $r$  as a function of [DTT]. The solid line is a linear fit to the data. Reproduced from ref 36. Copyright 2006 National Academy of Sciences, U.S.A.

tated because multiple events can be obtained in a single pulling trial. Furthermore, the error of pulling geometry and the histogram of the step height are less diversified in the case of polyproteins compared with their corresponding monomers.<sup>87</sup> Additionally, tandem repeats of many modules extend well over the region where nonspecific interactions between the polypeptide and the substrate are likely to happen and allow for a better signal-to-noise ratio.<sup>84</sup> In actual experiments, the tip can pick up a polyprotein from random positions. Consequently, in many (I27<sub>G32C-A75C</sub>)<sub>8</sub> recordings,  $<8$  domains are unfolded and a limited number of steps ranging from 1 to 8 are observed in the reduction regime (Figures 4 and 5). Although recordings with only one reduction step can, in principle, also be included in the ensemble for data analysis without impairing the accuracy of the measured rate, we recommend only traces with multiple reduction steps are used.

With these observations, we derive an empirical relationship  $r = k(F)[\text{DTT}]$ , where  $k(F)$  depends exponentially on the applied force:  $k(F) = A \exp((F\Delta x_r - E_a)/k_B T)$  (eq 1). Fitting  $\ln r$  versus  $F$  with a straight line, as shown in Figure 7A, we obtain  $\Delta x_r = 0.34$  Å from the slope and  $k(0) = 6.54 \text{ M}^{-1} \text{ s}^{-1}$  from the extrapolation, which

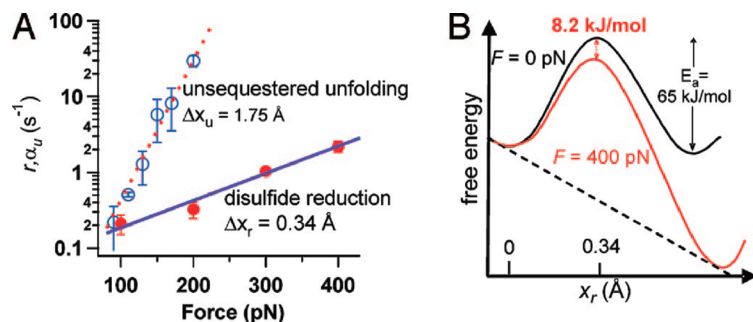


**Figure 7.** Force sensitivity in the thiol/disulfide exchange reaction. (A) Semilogarithmic plot of the rate of thiol/disulfide exchange,  $r$  (filled circles), and of the unsequestered unfolding rate,  $\alpha_u$  (open circles), as a function of the pulling force. The solid line is a fit of the equation  $r = A(\exp((F\Delta x_r - E_a)/k_B T))[DTT]$ . The dashed line fits the unsequestered unfolding rate with  $\alpha_u(F) = \alpha_u(0)\exp(F\Delta x_u/k_B T)$ . (B) Illustration of the energy landscape of the thiol/disulfide exchange reaction under force. Reproduced from ref 36. Copyright 2006 National Academy of Sciences, U.S.A.

is similar to the rate constant for DTT reduction of disulfide bonds in insulin at neutral pH ( $k = 5 \text{ M}^{-1} \text{ s}^{-1}$ ).<sup>92</sup> The applied force alters the rate constant in our system;  $k(200 \text{ pN}) = 27.6 \text{ M}^{-1} \text{ s}^{-1}$ , a 4-fold increase from zero force. Each 100 pN of force lowers the energy barrier by  $\sim 2 \text{ kJ/mol}$  (Figure 7B). Compared with the calculated energy barrier of thiol/disulfide reactions in solution (60–66 kJ/mol),<sup>93</sup> a force of 400 pN lowers the barrier by  $\sim 12\%$ .

Following the same data analysis process, we can fit a single exponential to an average of traces containing solely unsequestered unfolding events of  $(I27_{G32C-A75C})_8$  that happen during the first force pulse and measure the rate of unfolding,  $\alpha_u = 1/\tau_u$ , at different pulling forces. Figure 7A also shows a semilogarithmic plot of  $\alpha_u$  as a function of the pulling force. The dashed line corresponds to a fit of  $\alpha_u(F) = \alpha_u(0)\exp(F\Delta x_u/k_B T)$ ,<sup>85</sup> obtaining  $\Delta x_u = 1.75 \text{ \AA}$  for the unsequestered unfolding. Here we assume the Markovian behavior for both the unfolding and reduction events, although there is also evidence that the extension of polyubiquitin resulting from unfolding slightly deviates from a simple exponential increase.<sup>86</sup> Figure 7A confirms the difference in force sensitivity between the unfolding and the thiol/disulfide exchange reaction, which are two distinct processes occurring within the same protein.

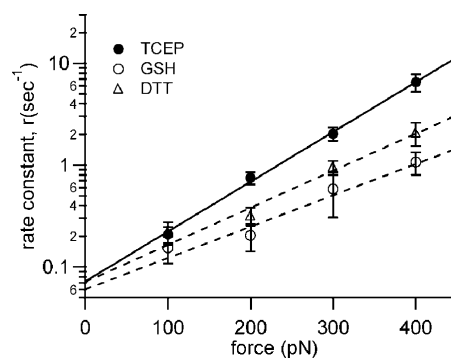
**Effect of Different Nucleophiles and Solvent.** In a recent survey, we performed single-molecule force spectroscopy studies on disulfide bond cleavage by various reducing agents, some of which are biologically active molecules.<sup>94</sup> The results are summarized in Table 1. The rates of all the reactions have first-order dependence on the concentration of the reducing agent and exponential dependence on stretching force. Interestingly, these thiol-based reducing agents have rather narrowly distributed values of  $\Delta x_r$  (0.29–0.35  $\text{\AA}$ ) except cysteine, which has a smaller  $\Delta x_r$  (0.23  $\text{\AA}$ ). Such similarity in  $\Delta x_r$  suggests that the transition states of disulfide bond reduction by these thiol-based reducing agents

probably have structurally and energetically common characteristics. For phosphine-based reducing agents TCEP and THP,  $\Delta x_r = 0.46 \pm 0.03$  and  $0.42 \pm 0.06 \text{ \AA}$ , respectively, which are larger than that of thiol-based reducing agents (Table 1 and Figure 8). These experimental results suggest that phosphine- and thiol-initiated reduction reactions have different characteristics related to their transition states.

It has been well-established that solvent can mediate the transition state of a chemical reaction or protein unfolding not only in bulk phase<sup>95–97</sup> but also in single-molecule force experiments.<sup>44,98</sup> We have performed disulfide bond reduction experiments by DTT and TCEP in a PBS buffer containing 30% v/v glycerol, and the results are shown in Figure 9, indicating that the effect of glycerol

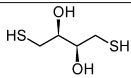
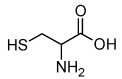
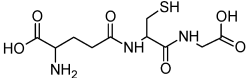
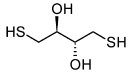
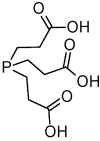
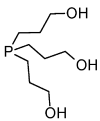
on each reaction is markedly different. For DTT, the glycerol halves the rate at each force up to 400 pN, but the slope of the force dependency,  $\Delta x_r$ , remains constant. On the other hand, for TCEP, addition of glycerol decreases the  $\Delta x_r$  from  $0.46 \pm 0.03$  to  $0.28 \pm 0.04 \text{ \AA}$ , while the extrapolations of the rates converge at zero force. These results suggest that the nature of the solvent affects in very different manners the route to the transition state for TCEP- and DTT-initiated reduction reactions under force. This phenomenon could be attributed to changes in the energetics, in the presence and absence of force, of the reactants as well as the transition states because of solvation<sup>99–104</sup> resulting from the different hydrogen-bonding properties for glycerol and water.<sup>105</sup> In addition, the relatively bulky glycerol molecules might affect the arrangement and the number of solvent molecules around the attacking and leaving groups in the transition state. Future studies involving a systematic change in the composition of glycerol/water mixture or other solvent mixtures, together with theoretical simulations, are necessary to give further insight into this issue.

**Physical Meaning of  $\Delta x_r$ .** The  $\Delta x_r$  value is obtained from the linear fitting of logarithmic rate *versus* force (Fig-



**Figure 8.** Arrhenius model fits to the force-dependent rate constants,  $r(F)$ , for different reducing agents. The steeper slope for phosphine indicates a higher force sensitivity and hence a larger  $\Delta x_r$ . Reproduced from ref 94. Copyright 2008 American Chemical Society.

TABLE 1. Disulfide Reduction by Different Reducing Agents<sup>a</sup>

disulfide reducing agent	structure	$\Delta x_r$ (Å)
DTT (1, 4-DL-dithiothreitol)		$0.34 \pm 0.05$
L-cysteine		$0.23 \pm 0.05$
GSH (L-Glutathione)		$0.29 \pm 0.06$
DTE (1, 4-dithioerythritol)		$0.33 \pm 0.05$
BME (β-mercaptoethanol)		$0.35 \pm 0.05$
TCEP (tris(2-carboxyethyl)phosphine)		$0.46 \pm 0.03$
THP (tris(hydroxypropyl)phosphine)		$0.42 \pm 0.06$

<sup>a</sup>Reproduced from ref 94. Copyright 2008 American Chemical Society.

ures 6–9) in the single-molecule force-clamp experiments. This fitting should only be carried out in the low force regime ( $F\Delta x_r \ll E_a$ ), however, because both theoretical<sup>106</sup> and experimental<sup>107</sup> approaches have revealed possible deviations from the linear response at high force. Recently, we discovered that protein disulfide bond cleavage by hydroxide anions exhibited an abrupt reactivity “switch” at  $\sim 500$  pN, after which the accelerating effect of force on the rate was greatly diminished.<sup>107</sup> It is also worth noting that the  $\Delta x_r$  is applicable for both protein unfolding and disulfide bond reduction processes (Figure 7A). Usually, the  $\Delta x_r$  for protein unfolding is significantly larger than that for disulfide bond reduction,<sup>36,85</sup> which can be understood from the fact that the structural deformation (elongation) of a folded protein as a whole up to the transition state is more dramatic than a single bond.

Compared with the  $A$  and  $E_a$  in the Arrhenius equation, which have long been studied,  $\Delta x_r$  is a new parameter and never before observed by other techniques. The force constant for a S–S bond, calculated from

its vibrational spectrum in the gas phase, is  $\sim 500$  N/m.<sup>108</sup> As a result, an applied force of 400 pN can stretch this bond by only 0.008 Å, which is a negligible effect on the geometry of the S–S bond and far less than our measured  $\Delta x_r$ . However, as pointed out by Beyer,<sup>109</sup> the reactivity of a stretched molecule is likely to depend on the pulling force despite only minor changes in bond geometry. Furthermore, a reorganiza-

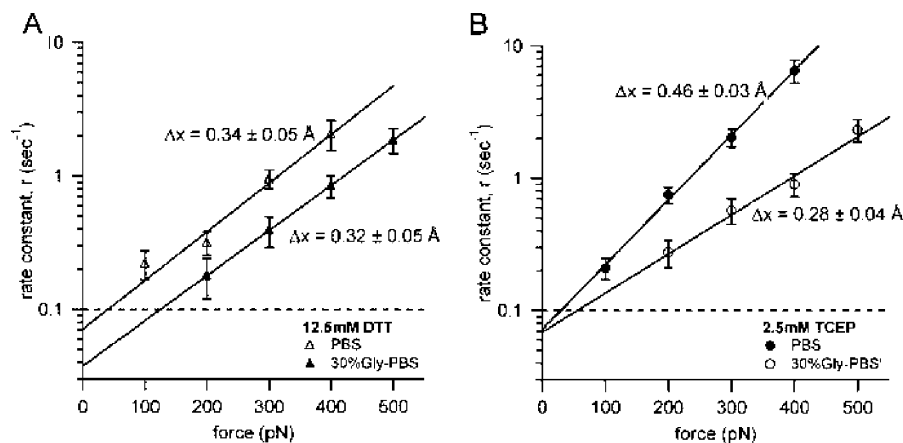
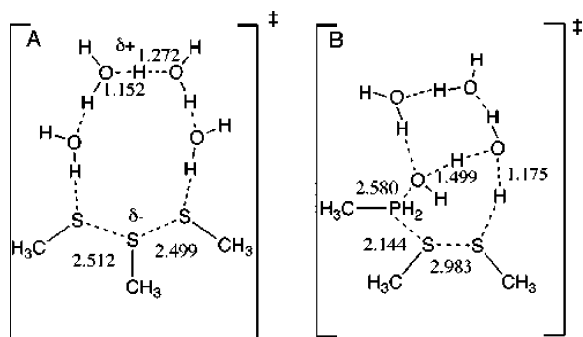


Figure 9. Comparison of the force-dependent rate in aqueous and glycerol solutions. (A) Rates of the disulfide bond reduction by DTT. Fitting with the Arrhenius model (solid line) gives  $\Delta x_r$ , which is barely changed. (B) When changing the solvent from aqueous to 30% v/v glycerol, the  $\Delta x_r$  decreases from 0.46  $\pm$  0.03 to 0.28  $\pm$  0.04 Å for TCEP-initiated disulfide bond reductions. Reproduced from ref 94. Copyright 2008 American Chemical Society.



**Figure 10.** Geometries of the transition states found for the prototypical reduction by (A) a thiol and (B) a phosphine including the aqueous environment. Bond distances are in angstroms. Reproduced from ref 94. Copyright 2008 American Chemical Society.

tion of the energy landscape of the bond is likely to occur during bond lengthening.<sup>110</sup> Recent theoretical calculations have proposed that the length of a S–S bond at the transition state of a simple  $S_N2$  thiol/disulfide exchange reaction in solution increases by 0.36 Å.<sup>111</sup> These values are close to the  $\Delta x_r$  we have measured experimentally with DTT. However, in some theoretical studies, the S–S lengthening at the transition state can be as small as 0.24 Å or as large as 0.78 Å.<sup>93</sup> Despite the complex and still controversial nature of this parameter, we can still extract useful information from our analysis, especially with the help of theoretical simulations.

To investigate the transition states of disulfide bond reduction by phosphines and thiols, as have been discussed above, we perform quantum chemical calculations on the basis of the model of Fernandes and Ramos.<sup>93</sup> Because the simulation is computationally intense, we use a simplified reaction to represent the highly complex system, including the following reactants in the presence of four extra water molecules:

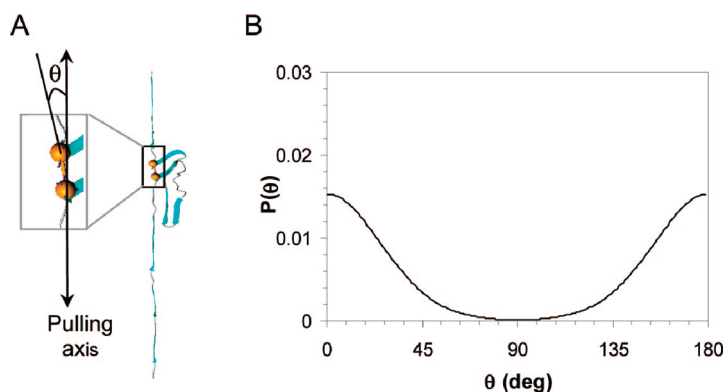
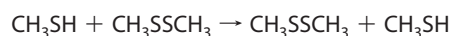


**Figure 11.** (A) Cartoon showing the unfolded protein with disulfide bond under mechanical force, in which the disulfide bond is oriented at an angle  $\theta$  with respect to the pulling axis. (B) Probability density function,  $P(\theta)$ , of disulfide bond orientation,  $\theta$ , calculated using the freely jointed chain model. Reproduced from ref 94. Copyright 2008 American Chemical Society.

At the transition state (Figure 10), the key feature is that the disulfide bond length to be broken for phosphine-initiated reduction is 2.983 Å, which is significantly longer than the corresponding bond length for thiol-initiated reduction of 2.499 Å. The S–S bond distance in dimethyl disulfide is 2.090 Å prior to reaction. Thus, we find qualitative agreement between the experimental data and the quantum chemical calculations in terms of the transition state geometry, although a number of factors need to be considered to gain full quantitative accordance. For instance, one of the errors may come from the fact that the disulfide bond in the stretched polypeptide is not fully aligned with the pulling axis. We use a freely jointed chain (FJC) model of polymer elasticity to estimate the distribution of disulfide bond orientations,  $\theta$ , with respect to the pulling axis.<sup>94</sup> The probability density function,  $P(\theta)$ , gives the distribution of  $\theta$  as below:

$$P(\theta) = \frac{e^{[Fb|\cos(\theta)]/[k_B T]}}{\int_0^{180} e^{[Fb|\cos(\theta)]/[k_B T]} d\theta} \quad (3)$$

where  $\theta = [0, 180]$ ,  $b = 2.09$  Å is the quantum chemically calculated disulfide bond length,  $k_B$  is Boltzmann's constant, and  $T = 298$  K is the absolute temperature. We define  $\theta = 90^\circ$  as the angle perpendicular to the pulling direction. The probability of disulfide bond orienting away from the pulling axis decreases from 0 to  $90^\circ$  (Figure 11). After incorporating this model, the calculated  $\Delta x_r$  for thiol is in agreement with the experimental value, but for phosphines, the theoretical and experimental values are still controversial.<sup>94</sup> In the latter case, the steric factors resulting from the bulky functional groups on the nucleophilic center of TCEP or THP (see Table 1 for structures) may limit the directions along which the phosphines approach the disulfide bond. Future studies, taking all the above factors into consideration, should lead to a more quantitative agreement between the experiments and calculations.

In summary, the  $\Delta x_r$  value is a measure of the effect of force on the reaction rate in single-molecule force-clamp spectroscopy. Straightforwardly, the activation energy barrier of the process (disulfide bond reduction or protein unfolding) is lowered by  $F\Delta x_r$ , but there is difficulty when directly correlating  $\Delta x_r$  with the actual bond elongation or deformation of the protein at their transition states. Many factors, including the deviation of the stretching force from the bond axis, the solvent effect, and the dynamic nature of the molecule to its transition state, should be considered comprehensively. For instance, in a typical  $S_N2$  reaction, the electron-deficient center undergoes an umbrella-like inversion during which the bond angles are continuously changing, adding much complexity to the system. Therefore,

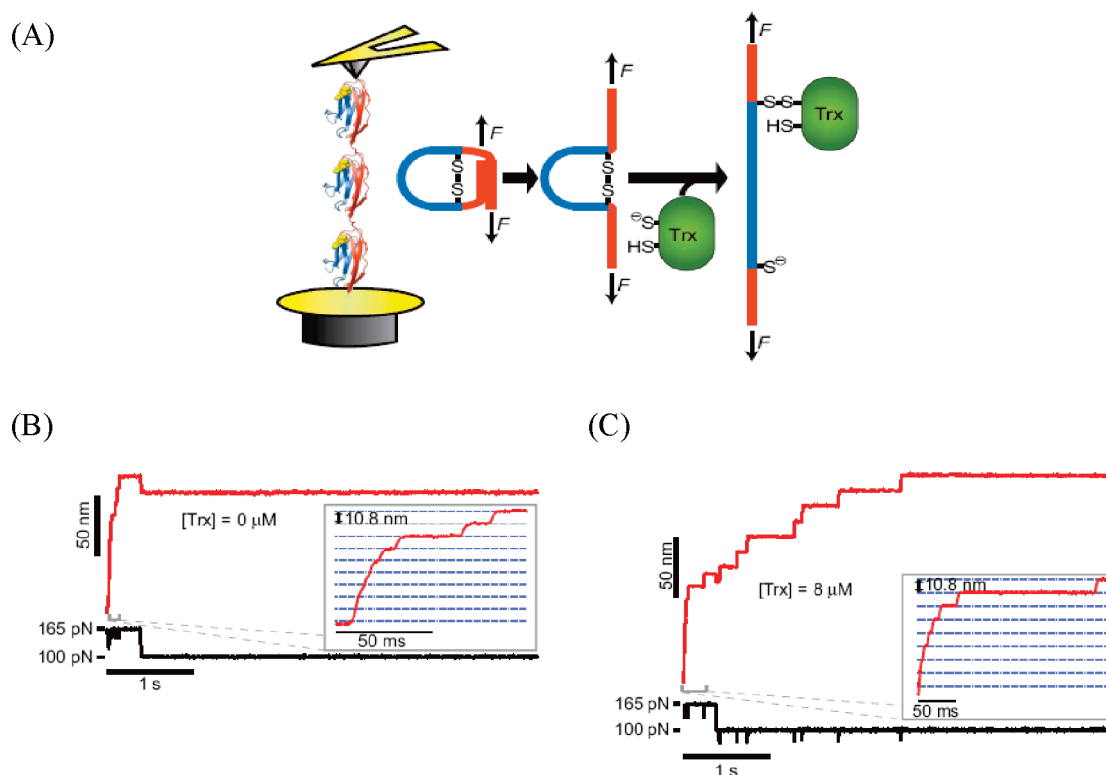


**Figure 12.** Identification of single Trx catalytic events. (A) Single (I27<sub>G32C–A75C</sub>)<sub>8</sub> molecules are stretched using an AFM in force-clamp mode (left). After unfolding of the red residues, the disulfide bond is exposed to the solution. On disulfide reduction by Trx, the blue residues previously trapped behind the disulfide bond are immediately extended. (B) Single (I27<sub>G32C–A75C</sub>)<sub>8</sub> molecule is stretched in the absence of Trx. No further steps are noted during the second pulse of 100 pN. (C) In the presence of 8 mM Trx, seven steps of 13.2 nm are observed during the second pulse, corresponding to the extension of the trapped residues in each module after the reduction of individual disulfide bonds by Trx enzymes. Reproduced from ref 115. Copyright 2007 Nature Publishing Group.

$\Delta x_r$ , probably should be considered an “overall” bond elongation effect along the reaction coordinate. Further experimental and theoretical advances on the elucidation of the meaning of  $\Delta x_r$  will certainly provide new insight into the force effect on chemical reactions.

#### Disulfide Bond Reduction Reactions by Enzymes

**(Thioredoxins).** Thioredoxin (Trx) is an oxidoreductase enzyme which is ubiquitous and essential for life in nearly all known organisms, from plants to bacteria and mammals.<sup>112,113</sup> Thioredoxins typically act as antioxidants by reducing disulfide bonds in other proteins through thiol/disulfide exchange. Thioredoxins are characterized by the presence of two vicinal cysteines in a Cys-X-X-Cys motif, which are the key to their thiol/disulfide exchange ability.<sup>114</sup> The effect of force (stress) on the substrate, that is, the activity of thioredoxins on a stretched disulfide bond, however, had never been reported. Recently, we monitored the *E. coli* Trx-catalyzed reduction of individual disulfide bonds in (I27<sub>G32C–A75C</sub>)<sub>8</sub> placed under the two-pulse force discussed above.<sup>115</sup> After unfolding, the stretching force is applied directly to the disulfide bond, and if Trx is present in solution, the bond can be chemically reduced by the enzyme (Figure 12).

Figure 13 shows a plot of the reaction rate as a function of the applied force. Remarkably, the rate of reduc-

tion decreases 4-fold between 25 and 250 pN, and then increases approximately 3-fold when the force is increased up to 600 pN, demonstrating a biphasic force dependency. This result is in contrast with the uniform acceleration of reduction rate with increasing force by DTT, TCEP, or other small nucleophiles, underlining a more complex reaction mechanism catalyzed by Trx. We describe the force-resistant and force-favored regimes as two separate pathways for the disulfide bond reduction by Trx. Another way of data processing, called dwell time analysis, also confirms the presence of the two pathways.<sup>116</sup> Furthermore, unlike the linear response of the rate to the concentration of small nucleophiles, the rate of reduction becomes saturated at relatively high concentration of Trx (Figure 13C). An extrapolation to zero force in Figure 13B predicts a rate constant for Trx reduction of  $2.2 \times 10^5 \text{ M}^{-1} \text{ s}^{-1}$ , which is  $\sim 30\,000$  times faster than that found for I27 disulfide reduction by DTT ( $6.5 \text{ M}^{-1} \text{ s}^{-1}$ ). This result is consistent with bulk biochemical experiments, in which Trx has been found to reduce insulin disulfide bonds  $\sim 20\,000$  times faster than DTT ( $1 \times 10^5 \text{ M}^{-1} \text{ s}^{-1}$  for Trx versus  $5 \text{ M}^{-1} \text{ s}^{-1}$  for DTT at pH 7),<sup>117</sup> indicating Trx, the biologically active enzyme, is a much more efficient reducing agent than small nucleophiles.

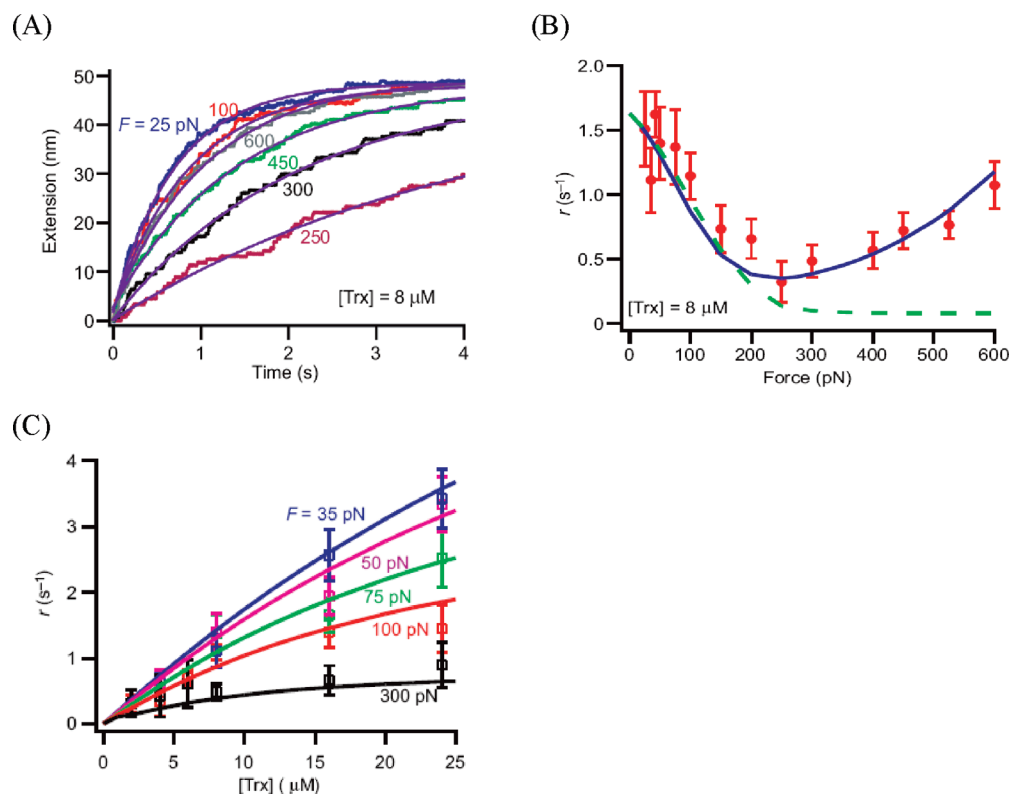


**Figure 13.** Force-dependent Trx catalysis. (A) Multiple ( $n = 10\text{--}30$ ) single-molecule recordings of the reduction events are averaged. A single exponential is fitted to each averaged trace (smooth line). (B) The  $r$  as a function of force at  $[\text{Trx}] = 8 \mu\text{M}$ . The plot indicates two modes of Trx catalysis under force. The dashed green line represents fits in the absence of the second pathway. (C) The  $r$  as a function of  $[\text{Trx}]$  at various forces. Reproduced from ref 115. Copyright 2007 Nature Publishing Group.

To explain the first reaction pathway, that is, why the rate decreases with the application of force onto the substrate disulfide bond, we assume the two pathways are independent of each other and each of them can be described by the straightforward Arrhenius term:  $r = \beta_0 \exp(F\Delta x_r/k_B T)$ , where  $\beta_0$  is the rate constant at zero force. By doing so, we obtain  $\Delta x_r = -0.79 \pm 0.09 \text{ \AA}$  for the catalytic path I (the left fork) and  $\Delta x_r = 0.17 \pm 0.02 \text{ \AA}$  for the catalytic path II (the right fork).<sup>115</sup> Thus, the two catalytic pathways are very different: the transition state of reduction by way of path I requires a shortening of the substrate polypeptide by  $\sim 0.8 \text{ \AA}$  (negative  $\Delta x_r$  value), whereas path II requires an elongation by  $\sim 0.2 \text{ \AA}$  (positive  $\Delta x_r$  value).

For DTT or TCEP, the bond is stretched and aligned with the force, and the small molecule can perform the nucleophilic attack without altering drastically this geometry. Therefore, the reaction rate is always force-favored because of the bond elongation along the pulling coordinate. Enzymatic catalysis, however, requires first the binding of enzyme to the substrate, which can lower the activation energy of the reaction by stabilizing the transition state (Michaelis–Menten kinetics). This binding may restrict the orientation of the disulfide bond with respect to the pulling force and the nucleophilic atom in the active site. A glimpse of the transition state for Trx catalysis can be referred from the

NMR structure of human Trx, a homologue of the *E. coli* Trx,<sup>118,119</sup> in a complex with a substrate peptide from the signaling protein NF- $\kappa$ B (Figure 14). In this structure, as well as in other similar structures,<sup>120</sup> a peptide-binding groove is identified on the surface of Trx in the vicinity of the catalytic Cys32. The sulfur atom in Cys32 (sulfur atom A) of the active site of Trx forms a disulfide bond with the sulfur atom of the NF- $\kappa$ B peptide (sulfur atom B). This configuration is in good accordance with the  $S_N2$  mechanism, which is highly directional, requiring the three involved sulfur atoms to form a  $\sim 180^\circ$  angle. Assuming that upon binding the sulfur atom of the catalytic Cys32 of Trx dramatically departs from the  $180^\circ$  angle position, the target disulfide bond must rotate with respect to the pulling axis to acquire the correct  $S_N2$  geometry of the transition state (Figure 14B). This starting geometry is supported by our theoretical modeling of the enzyme–disulfide bond complex.<sup>115</sup> This rotation is against the force because it requires a length shortening along the pulling direction. Therefore, our experiments actually show a sub-angstrom-level distortion of the substrate disulfide bond during Trx catalysis.

The origin of the  $\Delta x_r \sim 0.2 \text{ \AA}$  elongation of *E. coli* Trx catalysis, measured from the force dependency of path II, is less clear. However, molecular dynamics simulations have demonstrated other possible reaction ge-

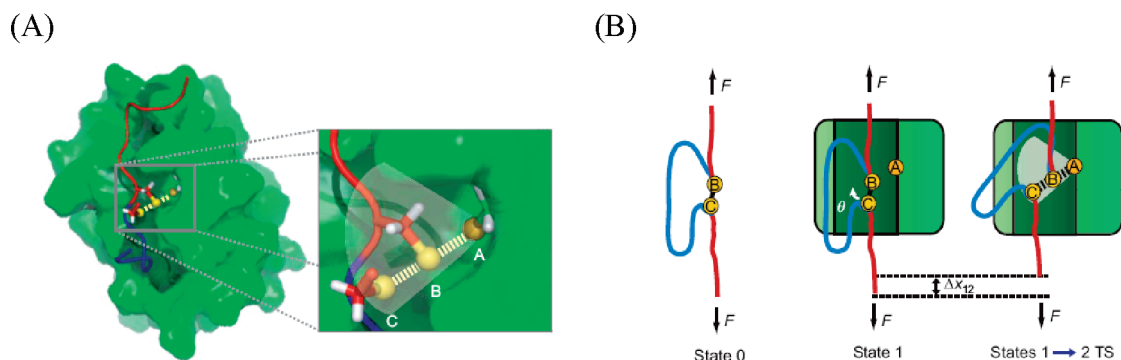


**Figure 14.** Structural model for force-dependent Trx catalysis. (A) Trx (peptide-binding groove in dark green) bound to a NF- $\kappa$ B peptide. The inset (yellow spheres are sulfur atoms A, B, and C) shows the relative position of the disulfide bond between Trx Cys32 (sulfur atom A) and the NF- $\kappa$ B cysteine (sulfur atom B). The third sulfur atom (sulfur atom C) belonging to the leaving cysteine is placed 180° from the disulfide bond, as required by the  $S_N2$  chemical reaction. (B) Cartoon representation of the reduction by Trx of a disulfide bond in a stretched polypeptide. On binding, the substrate disulfide bond (between sulfur atoms B and C) has to rotate by an angle  $\theta$  to acquire the correct  $S_N2$  geometry at the transition state of the reaction, causing a contraction of the substrate polypeptide by an amount  $\Delta x_{12}$ . This rotation is opposed by the pulling force. Reproduced from ref 115. Copyright 2007 Nature Publishing Group.

ometries of thiol/disulfide exchange.<sup>93,121,122</sup> Analogous to Figure 14B, we can imagine that the  $\Delta x_r$  can adopt various values if the catalytic Cys moves along an axis parallel to the disulfide bond; that is,  $\Delta x_r$  is likely to be negative if the catalytic Cys falls in a position between the two sulfur atoms of the disulfide bond or positive when the catalytic Cys is located at the far end. Therefore, the absolute value of  $\Delta x_r$  is likely correlated to the equilibrium position of the catalytic sulfur atom with respect to the disulfide bond upon binding.

It is interesting to test and compare the reactivities of thioredoxins from different species with the stretched disulfide bond. Recently, we combined statistical analysis of protein sequences with the sensitivity of single-molecule force-clamp spectroscopy to probe how catalysis is affected by structurally distant correlated mutations in *E. coli* thioredoxin.<sup>123</sup> Although it is not yet known how often a single disulfide bond *in vivo* is exposed to the force levels we explore in this study, it is likely that some particular thiol/disulfide exchange reactions are sensitive to a pulling force generated from the environment surrounding the bond. In our experiments, forces of  $\sim 100$  pN are enough to achieve a measurable increase in the rate of thiol/disulfide exchange which is within the range experienced in cell biology.<sup>124,125</sup> Particularly, in reactions where  $\Delta x_r$  is  $> 1$  Å, a near 2-fold increase in the reduction rate may appear upon just 20 pN of applied force, suggesting that force-catalyzed chemical reactions may play an important role *in vivo*.

Analogous to the engineered I27<sub>G32C–A75C</sub>, many natural proteins contain disulfide bonds that are buried in the hydrophobic core, as well. Mechanical force can partially unravel the protein and expose the disulfide bond to the redox environment. The reduction of the S–S bond leads to the completion of the unfolding of the whole protein module, which can trigger the biochemical signal of the next step. Indeed, the core disulfide bond can be solvent-exposed in the very earliest

stages of protein extension, as shown by molecular dynamics simulations on vascular cell adhesion protein,<sup>67</sup> suggesting that the redox state of a protein can be extremely sensitive to mechanical stress.

The correct functioning of some proteins may require the coexistence of mechanical tensions and active disulfide reductases. For instance, laminin, a trimeric protein in the basal membrane, has a number of interlocking disulfide bonds in its structure.<sup>126</sup> The basal membrane is normally subjected to the mechanical forces generated by the migration of endothelial cells. Meanwhile, thioredoxins are able to reduce the disulfide bonds in laminin,<sup>127</sup> implying that a regulation mechanism containing both mechanical and chemical switches might exist in the growth and survival of the basal membrane of vascular endothelium. Some experiments mimicking the redox and stretching conditions experienced by a protein *in vivo* have been reported, one of which is on Angiostatin (ANG),<sup>128,129</sup> a multimodular protein with disulfide bonds found on the basal membrane. In this approach, the pulling experiments were performed after the ANG being treated with human Trx at a concentration similar to that on the surface of mammalian tissues. Force-extension curves demonstrate that, under these conditions, the human Trx selectively reduces the Cys1–Cys78 disulfide bond, leading to a partially unfolded intermediate. Molecular simulations indicate that this intermediate has increased binding affinity with ATPases and may play important roles for the cell antimigratory activity, suggesting a regulation mechanism tuned by both force and chemistry.

## CONCLUSIONS

Using single-molecule force-clamp spectroscopy to study chemical reactions is an emerging field across the boundaries of physics, chemistry, and biology. Many techniques have the ability to probe one molecule at a time at ultralow pressures, such as mass spectroscopy, where

single ions are distinguished by their mass-to-charge ratios. However, in condensed phase, it was not until 1980s that single-molecule detection became possible, with the development of scanning probe microscopy,<sup>130,131</sup> fluorescence spectroscopy,<sup>132,133</sup> optical<sup>134,135</sup> and magnetic tweezers,<sup>22,136</sup> and surface-enhanced Raman spectroscopy.<sup>137,138</sup> In single-molecule force spectroscopy, AFM has been employed in probing the mechanical properties of polymers, DNAs, and proteins, but only recently, investigating the kinetics of chemical reactions on a single bond under constant stretching forces was reported. Taking advantage of the high resolution and low noise level of our custom-built AFM, we can perform single-molecule force-clamp spectroscopy on engineered polyproteins. The polyprotein has a well-known native structure and a well-defined disulfide bond forming a "loop" structure, which offers unambiguous fingerprints for the unfolding and thiol/disulfide exchange events at single-molecule level. Our work demonstrates that the rate of disulfide bond cleavage through an  $S_N2$  mechanism is dependent on the external force stretching the bond, and well described by an Arrhenius term of the form:  $r = A(\exp((F\Delta x_r - E_a)/k_B T))$  [nucleophile]. The fitting of the force dependency of the reduction rate gives a new variable,  $\Delta x_r$ , never been observed by other techniques. The  $\Delta x_r$  value is related to the bond elongation to the transition state during the mechanochemical reaction, which is an overall effect including many contributing factors, such as the specific nucleophile, the solvent molecules, and the dynamic motions of atoms in the local environment. Combined with theoretical simulations, we are able to obtain delicate information about the transition state of the reactions. We anticipate that mechanical activation of chemical reactions by force-clamp AFM will become an important tool in the chemist's arsenal to probe short-lived transition states in solution-phase reactions.

Mechanical stretching force can also affect the reactivity of a disulfide bond with thioredoxin enzymes, but in a more complex manner. The reaction rate for *E. coli* thioredoxin drops at low force regime but then increases when the force is higher than a certain threshold (~200 pN). The binding of the disulfide bond to the enzyme results in delicate structure of atoms on the active site, leading to necessary force-resistant or force-favored rearrangement of the bond to fulfill the required  $S_N2$  geometry. These observations may shed some light, at molecular level, onto a number of *in vivo* biological phenomena. For example, it is known that the increased mechanical stress during hypertension triggers an oxidative stress response in vascular endothelium and smooth muscle<sup>139</sup> that is compensated by an increase in the activity of thioredoxin.<sup>140,141</sup> In this context, single-molecule force spectroscopy may play an important role in understanding the fundamental mechanisms underlying enzymatic chemistry.

Although progress has been made from both experimental and theoretical sides, many questions are still open on the reactivity of a chemical bond under force. Carrying out force-clamp spectroscopic characterizations on other chemical bonds (besides disulfide) and on other types of reactions (besides  $S_N2$ ) will provide further insight into this emerging field. On the other hand, the experimental data and the theoretical models<sup>106,142–145</sup> are still far from quantitative agreement. Elucidation of the physical meaning of  $\Delta x_r$  and development of quantum mechanical simulations accepting mechanical force as a driving perturbation are some of the new challenges for theoretical chemists. Further goals for the application of force spectroscopy in biochemistry should involve the employment of this technique on proteins in living cells.<sup>146</sup>

**Acknowledgment.** We thank Dr. S. Garcia-Manyes, Dr. J. Alegre-Cebollada, Dr. A.P. Wiita, and other members of the Fernández laboratory for critical reading and helpful discussions of the manuscript. This work was supported by NIH Grants HL66030 and HL61228 (to J.M.F.).

## REFERENCES AND NOTES

- Beyer, M. K.; Clausen-Schaumann, H. Mechanochemistry: The Mechanical Activation of Covalent Bonds. *Chem. Rev.* **2005**, *105*, 2921–2948.
- Hickenboth, C. R.; Moore, J. S.; White, S. R.; Sottos, N. R.; Baudry, J.; Wilson, S. R. Biasing Reaction Pathways with Mechanical Force. *Nature* **2007**, *446*, 423–427.
- Osuna, S.; Swart, M.; Sola, M. The Diels–Alder Reaction on Endohedral  $Y_3N@C_{78}$ : The Importance of the Fullerene Strain Energy. *J. Am. Chem. Soc.* **2009**, *131*, 129–139.
- Huang, Z.; Yang, Q. Z.; Khvostichenko, D.; Kucharski, T. J.; Chen, J.; Boulatov, R. Method to Derive Restoring Forces of Strained Molecules from Kinetic Measurements. *J. Am. Chem. Soc.* **2009**, *131*, 1407–1409.
- Procyk, A. D.; Bocian, D. F. Vibrational Characteristics of Tetrapyrrolic Macrocycles. *Annu. Rev. Phys. Chem.* **1992**, *43*, 465–496.
- Atkins, P. W. *Physical Chemistry*; Oxford University Press: Oxford, 1995; pp 569–576.
- Azzaroni, O.; Trappmann, B.; van Rijn, P.; Zhou, F.; Kong, B.; Huck, W. T. S. Mechanically Induced Generation of Counterions Inside Surface-Grafted Charged Macromolecular Films: Towards Enhanced Mechanotransduction in Artificial Systems. *Angew. Chem., Int. Ed.* **2006**, *45*, 7440–7443.
- Paulusse, J. M. J.; Sijbesma, R. P. Reversible Mechanochemistry of a  $Pd^{II}$  Coordination Polymer. *Angew. Chem., Int. Ed.* **2004**, *43*, 4460–4462.
- Mehta, A. D.; Rief, M.; Spudich, J. A.; Smith, D. A.; Simmons, R. M. Single-Molecule Biomechanics with Optical Methods. *Science* **1999**, *283*, 1689–1695.
- Ritort, F. Single-Molecule Experiments in Biological Physics: Methods and Applications. *J. Phys.: Condens. Matter* **2006**, *18*, R531–R583.
- Neuman, K. C.; Attila, N. Single-Molecule Force Spectroscopy: Optical Tweezers, Magnetic Tweezers and Atomic Force Microscopy. *Nat. Methods* **2008**, *5*, 491–505.
- Herbert, K. M.; Greenleaf, W. J.; Block, S. M. Single-Molecule Studies of RNA Polymerase: Motoring along. *Annu. Rev. Biochem.* **2008**, *77*, 149–176.
- Grier, D. G. A Revolution in Optical Manipulation. *Nature* **2003**, *424*, 810–816.
- Wen, J.-D.; Laura, L.; Hodges, C.; Zeri, A.-C.; Yoshimura, S. H.; Noller, H. F.; Bustamante, C.; Tinoco, I. Following Translation by Single Ribosomes One Codon at a Time. *Nature* **2008**, *452*, 598–603.

15. Kollmannsberger, P.; Fabry, B. High-Force Magnetic Tweezers with Force Feedback for Biological Applications. *Rev. Sci. Instrum.* **2007**, *78*, 114301–114306.
16. Yan, J.; Skoko, D.; Marko, J. F. Near-Field-Magnetic-Tweezer Manipulation of Single DNA Molecules. *Phys. Rev. E* **2004**, *70*, 011905.
17. Engel, A.; Gaub, H. E. Structure and Mechanics of Membrane Proteins. *Annu. Rev. Biochem.* **2008**, *77*, 127–148.
18. Müller, D. J.; Dufre ne, Y. F. Atomic Force Microscopy as a Multifunctional Molecular Toolbox in Nanobiotechnology. *Nat. Nanotechnol.* **2008**, *3*, 261–269.
19. Hansma, H. G. Surface Biology of DNA by Atomic Force Microscopy. *Annu. Rev. Phys. Chem.* **2001**, *52*, 71–92.
20. Janshoff, A.; Neitzert, M.; Oberdorfer, Y.; Fuchs, H. Force Spectroscopy of Molecular Systems-Single Molecule Spectroscopy of Polymers and Biomolecules. *Angew. Chem., Int. Ed.* **2000**, *39*, 3213–3237.
21. Carrion-Vazquez, M.; Oberhauser, A. F.; Fisher, T. E.; Marszalek, P. E.; Li, H. B.; Fern andez, J. M. Mechanical Design of Proteins Studied by Single-Molecule Force Spectroscopy and Protein Engineering. *Prog. Biophys. Mol. Biol.* **2000**, *74*, 63–91.
22. Smith, S. B.; Finzi, L.; Bustamante, C. Direct Mechanical Measurements of the Elasticity of Single DNA Molecules by Using Magnetic Beads. *Science* **1992**, *258*, 1122–1126.
23. Rief, M.; Gautel, M.; Oesterhelt, F.; Fernandez, J. M.; Gaub, H. E. Reversible Unfolding of Individual Titin Immunoglobulin Domains by AFM. *Science* **1997**, *276*, 1109–1112.
24. Kellermayer, M. S. Z.; Smith, S. B.; Granzier, H. L.; Bustamante, C. Folding–Unfolding Transitions in Single Titin Molecules Characterized with Laser Tweezers. *Science* **1997**, *276*, 1112–1116.
25. Kufer, S. K.; Puchner, E. M.; Gump, H.; Liedl, T.; Gaub, H. E. Single-Molecule Cut-and-Paste Surface Assembly. *Science* **2008**, *319*, 594–596.
26. Lee, G.; Abdi, K.; Jiang, Y.; Michaelis, P.; Bennett, V.; Marszalek, P. E. Nanospring Behaviour of Ankyrin Repeats. *Nature* **2006**, *440*, 246–249.
27. Hugel, T.; Holland, N. B.; Cattani, A.; Moroder, L.; Seitz, M.; Gaub, H. E. Single-Molecule Optomechanical Cycle. *Science* **2002**, *296*, 1103–1106.
28. Ray, C.; Brown, J. R.; Kirkpatrick, A.; Akhremitchev, B. B. Pairwise Interactions between Linear Alkanes in Water Measured by AFM Force Spectroscopy. *J. Am. Chem. Soc.* **2008**, *130*, 10008–10018.
29. Junker, J. P.; Ziegler, F.; Rief, M. Ligand-Dependent Equilibrium Fluctuations of Single Calmodulin Molecules. *Science* **2009**, *323*, 633–637.
30. Borgia, A.; Williams, P. M.; Clarke, J. Single-Molecule Studies of Protein Folding. *Annu. Rev. Biochem.* **2008**, *77*, 101–125.
31. Sharma, D.; Cao, Y.; Li, H. Engineering Proteins with Novel Mechanical Properties by Recombination of Protein Fragments. *Angew. Chem., Int. Ed.* **2006**, *45*, 5633–5638.
32. Li, H.; Carrion-Vazquez, M.; Oberhauser, A. F.; Marszalek, P. E.; Fern andez, J. M. Point Mutations Alter the Mechanical Stability of Immunoglobulin Modules. *Nat. Struct. Biol.* **2000**, *7*, 1117–1120.
33. Chyan, C. L.; Lin, F. C.; Peng, H.; Yuan, J. M.; Chang, C. H.; Lin, S. H.; Yang, G. Reversible Mechanical Unfolding of Single Ubiquitin Molecules. *Biophys. J.* **2004**, *87*, 3995–4006.
34. Kersey, F. R.; Yount, W. C.; Craig, S. L. Single-Molecule force Spectroscopy of Bimolecular Reactions: System Homology in the Mechanical Activation of Ligand Substitution Reactions. *J. Am. Chem. Soc.* **2006**, *128*, 3886–3887.
35. Duwez, A. S.; Cuenot, S.; J er ome, C.; Gabriel, S.; J er ome, R.; Rapino, S.; Zerbetto, F. Mechanochemistry: Targeted Delivery of Single Molecules. *Nat. Nanotechnol.* **2006**, *1*, 122–125.
36. Wiita, A. P.; Ainaravaru, S. R. K.; Huang, H. H.; Fern andez, J. M. Force-Dependent Chemical Kinetics of Disulfide Bond Reduction Observed with Single-Molecule Techniques. *Proc. Natl. Acad. Sci. U.S.A.* **2006**, *103*, 7222–7227.
37. Grandbois, M.; Beyer, M.; Rief, M.; Clausen-Schaumann, H.; Gaub, H. E. How Strong Is a Covalent Bond? *Science* **1999**, *283*, 1727–1730.
38. Schwaderer, P.; Funk, E.; Achenbach, F.; Weis, J.; Br auchle, C.; Michaelis, J. Single-Molecule Measurement of the Strength of a Siloxane Bond. *Langmuir* **2008**, *24*, 1343–1349.
39. Lupton, E. M.; Nonnenberg, C.; Frank, I.; Achenbach, F.; Weis, J.; Brauchle, C. Stretching Siloxanes: An *Ab Initio* Molecular Dynamics Study. *Chem. Phys. Lett.* **2005**, *414*, 132–137.
40. Kamper, S. G.; Porter-Peden, L.; Blankespoor, R.; Sinniah, K.; Zhou, D. J.; Abell, C.; Rayment, T. Investigating the Specific Interactions between Carbonic Anhydrase and a Sulfonamide Inhibitor by Single-Molecule Force Spectroscopy. *Langmuir* **2007**, *23*, 12561–12565.
41. Lee, G. U.; Chrisley, L. A.; Colton, R. J. Direct Measurement of the Forces between Complementary Strands of DNA. *Science* **1994**, *266*, 771–773.
42. Moy, V. T.; Florin, E. L.; Gaub, H. E. Intermolecular Forces and Energies between Ligands and Receptors. *Science* **1994**, *266*, 257–259.
43. Ke, C.; Humeniuk, M.; S-Gracz, H.; Marzalek, P. E. Direct Measurement of Base Stacking Interactions in DNA by Single-Molecule Atomic-Force Spectroscopy. *Phys. Rev. Lett.* **2007**, *99*, 018302.
44. Dougan, L.; Ainaravaru, S. R. K.; Genchev, G.; Lu, H.; Fern andez, J. M. A Single-Molecule Perspective on the Role of Solvent Hydrogen Bonds in Protein Folding and Chemical Reactions. *ChemPhysChem* **2008**, *9*, 2836–2847.
45. Sotomayor, M.; Schulten, K. Single-Molecule Experiments *In Vitro* and *In Silico*. *Science* **2007**, *316*, 1144–1148.
46. Li, H.; Liu, B.; Zhang, X.; Gao, C.; Shen, J.; Zou, G. Single-Molecule Force Spectroscopy on Poly(acrylic acid) by AFM. *Langmuir* **1999**, *15*, 2120–2124.
47. Scherer, A.; Zhou, C.; Michaelis, J.; Brauchle, C.; Zumbusch, A. Intermolecular Interactions of Polymer Molecules Determined by Single-Molecule Force Spectroscopy. *Macromolecules* **2005**, *38*, 9821–9825.
48. Walther, K. A.; Bruji c, J.; Li, H.; Fern andez, J. M. Sub-Angstrom Conformational Changes of a Single Molecule Captured by AFM Variance Analysis. *Biophys. J.* **2006**, *90*, 3806–3812.
49. Marko, J. F.; Siggia, E. D. Stretching DNA. *Macromolecules* **1995**, *28*, 8759–8770.
50. Perkins, T. T.; Smith, D. E.; Chu, S. Single Polymer Dynamics in an Elongational Flow. *Science* **1997**, *276*, 2016–2021.
51. Fern andez, J. M.; Li, H. Force-Clamp Spectroscopy Monitors the Folding Trajectory of a Single Protein. *Science* **2004**, *303*, 1674–1678.
52. Oberhauser, A. F.; Hansma, P. K.; Carrion-Vazquez, M.; Fern andez, J. M. Stepwise Unfolding of Titin under Force-Clamp Atomic Force Microscopy. *Proc. Natl. Acad. Sci. U.S.A.* **2001**, *98*, 468–472.
53. Linke, W. A.; Gr utzner, A. Pulling Single Molecules of Titin by AFM-Recent Advances and Physiological Implications. *Eur. J. Physiol.* **2008**, *456*, 101–115.
54. Favre, M.; Sekatskii, S. K.; Dietler, G. Single-Molecule Avidin-Biotin Association Reaction Studied by Force-Clamp Spectroscopy. *Ultramicroscopy* **2008**, *108*, 1135–1139.
55. Samori, B.; Zuccheri, G.; Baschieri, P. Protein Unfolding and Refolding under Force: Methodologies for Nanomechanics. *ChemPhysChem* **2005**, *6*, 29–34. <http://fernandezlab.biology.columbia.edu/publications>.
56. Schmidt, B.; Hogg, P. J. Search for Allosteric Disulfide Bonds in NMR Structures. *BMC Struct. Biol.* **2007**, *7*, 49–60.
57. Matsumura, M.; Signor, G.; Matthews, B. W. Substantial Increase of Protein Stability by Multiple Disulphide Bonds. *Nature* **1989**, *342*, 291–293.
58. Wedemeyer, W. J.; Welker, E.; Narayan, M.; Scheraga, H. A. Disulfide Bonds and Protein Folding. *Biochemistry* **2000**, *39*, 4207–4216.

60. Shimaoka, M.; Lu, C. F.; Palframan, R. T.; von Andrian, U. H.; McCormack, A.; Takagi, J.; Spring, T. A. Reversibly Locking a Protein Fold in an Active Conformation with a Disulfide Bond: Integrin  $\alpha$  I Domains with High Affinity and Antagonist Activity *In Vivo*. *Proc. Natl. Acad. Sci. U.S.A.* **2001**, *98*, 6009–6014.
61. Wu, J.; Watson, J. T. A Novel Methodology for Assignment of Disulfide Bond Pairings in Proteins. *Protein Sci.* **1997**, *6*, 391–398.
62. Cline, D. J.; Redding, S. E.; Brohawn, S. G.; Psathas, J. N.; Schneider, J. P.; Thorpe, C. New Water-Soluble Phosphines as Reductants of Peptide and Protein Disulfide Bonds: Reactivity and Membrane Permeability. *Biochemistry* **2004**, *43*, 15195–15203.
63. Molinari, M.; Helenius, A. Glycoproteins form Mixed Disulphides with Oxidoreductases during Folding in Living Cells. *Nature* **1999**, *402*, 90–93.
64. Tu, B. P.; Ho-Schleyer, S. C.; Traver, K. J.; Weissman, J. S. Biochemical Basis of Oxidative Protein Folding in the Endoplasmic Reticulum. *Science* **2000**, *290*, 1571–1574.
65. Boggon, T. J.; Murray, J.; Chappuis-Flament, S.; Wong, E.; Gumbiner, B. M.; Shapiro, L. C-Cadherin Ectodomain Structure and Implications for Cell Adhesion Mechanisms. *Science* **2002**, *296*, 1308.
66. Graves, B. J.; Crowther, R. L.; Chandran, C.; Rumberger, J. M.; Li, S.; Huang, K. S.; Presky, D. H.; Familletti, P. C.; Wolitzky, B. A.; Burns, D. K. Insight into E-Selectin/Ligand Interaction from the Crystal Structure and Mutagenesis of the IEC/EGF Domains. *Nature* **1994**, *367*, 532–538.
67. Bhasin, N.; Carl, P.; Harper, S.; Feng, G.; Lu, H.; Speicher, D. W.; Discher, D. E. Chemistry on a Single Protein, Vascular Cell Adhesion Molecule-1, during Forced Unfolding. *J. Biol. Chem.* **2004**, *279*, 45865–45874.
68. Wierzbicka-Patynowski, I.; Schwarzbauer, J. E. The Ins and Outs of Fibronectin Matrix Assembly. *J. Cell Sci.* **2003**, *116*, 3269–3276.
69. Schrijver, I.; Liu, W.; Brenn, T.; Furthmayr, H.; Francke, U. Cysteine Substitutions in Epidermal Growth Factor-like Domains of Fibrillin-1: Distinct Effects on Biochemical and Clinical Phenotypes. *Am. J. Hum. Genet.* **1999**, *65*, 1007–1020.
70. Mayans, O.; Wuerges, J.; Canela, S.; Gautel, M.; Wilmanns, M. Structural Evidence for a Possible Role of Reversible Disulphide Bridge Formation in the Elasticity of the Muscle Protein Titin. *Structure* **2001**, *9*, 331–340.
71. Vogel, V. Mechanotransduction Involving Multimodular Proteins: Converting Force into Biochemical Signals. *Annu. Rev. Biophys. Biomol. Struct.* **2006**, *35*, 459–488.
72. Valle, F.; Sandal, M.; Samori, B. The Interplay between Chemistry and Mechanics in the Transduction of a Mechanical Signal into a Biochemical Function. *Phys. Life Rev.* **2007**, *4*, 157–188.
73. Bell, G. I. Models for the Specific Adhesion of Cells to Cells. *Science* **1978**, *200*, 618–627.
74. Hanggi, P.; Talkner, P.; Borkovec, M. Reaction-Rate Theory: Fifty Years after Kramers. *Rev. Mod. Phys.* **1990**, *62*, 251–341.
75. Evans, E. Probing the Relation between Force-Lifetime and Chemistry in Single Molecular Bonds. *Annu. Rev. Biophys. Biomol. Struct.* **2001**, *30*, 105–128.
76. Carl, P.; Kwok, C. H.; Manderson, G.; Speicher, D. W.; Discher, D. E. Forced Unfolding Modulated by Disulfide Bonds in the Ig Domains of a Cell Adhesion Molecule. *Proc. Natl. Acad. Sci. U.S.A.* **2001**, *98*, 1565–1570.
77. Bustanji, Y.; Samori, B. The Mechanical Properties of Human Angiostatin Can Be Modulated by Means of Its Disulfide Bonds: A Single-Molecule Force-Spectroscopy Study. *Angew. Chem., Int. Ed.* **2002**, *41*, 1546–1548.
78. Fisher, T. E.; Oberhauser, A. F.; Carrion-Vazquez, M.; Marszalek, P. E.; Fernández, J. M. The Study of Protein Mechanics with the Atomic Force Microscope. *Trends Biochem. Sci.* **1999**, *24*, 379–384.
79. Improta, S.; Politou, A.; Pastore, A. Immunoglobulin-like Modules from Titin I-Band: Extensible Components of Muscle Elasticity. *Structure* **1996**, *4*, 323–337.
80. Lu, H.; Isralewitz, B.; Krammer, A.; Vogel, V.; Schulten, K. Unfolding of Titin Immunoglobulin Domains by Steered Molecular Dynamics Simulation. *Biophys. J.* **1998**, *75*, 662–671.
81. Lu, H.; Schulten, K. Steered Molecular Dynamics Simulation of Conformational Changes of Immunoglobulin Domain I27 Interpret Atomic Force Microscopy Observations. *Chem. Phys.* **1999**, *247*, 141–153.
82. Lu, H.; Schulten, K. The Key Event in Force-Induced Unfolding of Titin's Immunoglobulin Domains. *Biophys. J.* **2000**, *79*, 51–65.
83. Gao, M.; Lu, H.; Schulten, K. Simulated Refolding of Stretched Titin Immunoglobulin Domains. *Biophys. J.* **2001**, *81*, 2268–2277.
84. Carrion-Vazquez, M.; Oberhauser, A. F.; Fowler, S. B.; Marszalek, P. E.; Broedel, S. E.; Clarke, J.; Fernández, J. M. Mechanical and Chemical Unfolding of a Single Protein: A Comparison. *Proc. Natl. Acad. Sci. U.S.A.* **1999**, *96*, 3694–3699.
85. Schlierf, M.; Li, H.; Fernández, J. M. The Unfolding Kinetics of Ubiquitin Captured with Single-Molecule Force-Clamp Techniques. *Proc. Natl. Acad. Sci. U.S.A.* **2004**, *101*, 7299–7304.
86. Brujić, J.; Hermans, R. I. Z.; Walther, K. A.; Fernández, J. M. Single-Molecule Force Spectroscopy Reveals Signatures of Glassy Dynamics in the Energy Landscape of Ubiquitin. *Nat. Phys.* **2006**, *2*, 282–286.
87. Garcia-Manyes, S.; Brujić, J.; Badilla, C. L.; Fernández, J. M. Force-Clamp Spectroscopy of Single-Protein Monomers Reveals the Individual Unfolding and Folding Pathways of I27 and Ubiquitin. *Biophys. J.* **2007**, *93*, 2436–2446.
88. Fisher, T. E.; Marszalek, P. E.; Oberhauser, A. F.; Carrion-Vazquez, M.; Fernández, J. M. The Micro-Mechanics of Single Molecules Studied with Atomic Force Microscopy. *J. Physiol.* **1999**, *520*, 5.
89. Cleland, W. W. Dithiothreitol, a New Protective Reagent for SH Groups. *Biochemistry* **1964**, *3*, 480–482.
90. Thaxton, C. S.; Hill, H. D.; Georganopoulou, D. G.; Stoeva, S. I.; Mirkin, C. A. A Bio-Bar-Code Assay Based upon Dithiothreitol-Induced Oligonucleotide Release. *Anal. Chem.* **2005**, *77*, 8174–8178.
91. Ainavarapu, S. R. K.; Wiita, A. P.; Huang, H. H.; Fernández, J. M. A Single-Molecule Assay to Directly Identify Solvent-Accessible Disulfide Bonds and Probe Their Effect on Protein Folding. *J. Am. Chem. Soc.* **2008**, *130*, 436–437.
92. Holmgren, A. Thioredoxin Catalyzes the Reduction of Insulin Disulfides by Dithiothreitol and Dihydroliipoamide. *J. Biol. Chem.* **1979**, *254*, 9627–9632.
93. Fernandes, P. A.; Ramos, M. J. Theoretical Insights into the Mechanism for Thiol/Disulfide Exchange. *Chem.—Eur. J.* **2004**, *10*, 257–266.
94. Ainavarapu, S. R. K.; Wiita, A. P.; Dougan, L.; Uggerud, E.; Fernández, J. M. Single-Molecule Force Spectroscopy Measurements of Bond Elongation during a Bimolecular Reaction. *J. Am. Chem. Soc.* **2008**, *130*, 6479–6487.
95. Heitele, H. Dynamic Solvent Effects on Electron-Transfer Reactions. *Angew. Chem., Int. Ed. Engl.* **1993**, *32*, 359–377.
96. Dill, K. A.; Shortle, D. Denatured States of Proteins. *Annu. Rev. Biochem.* **1991**, *60*, 795–825.
97. de Boeij, W. P.; Pshenichnikov, M. S.; Wiersma, D. A. Ultrafast Solvation Dynamics Explored by Femtosecond Photon Echo Spectroscopies. *Annu. Rev. Phys. Chem.* **1998**, *49*, 99–123.
98. Dougan, L.; Feng, G.; Lu, H.; Fernández, J. M. Solvent Molecules Bridge the Mechanical Unfolding Transition State of a Protein. *Proc. Natl. Acad. Sci. U.S.A.* **2008**, *105*, 3185–3190.
99. Buncel, E.; Wilson, H. Initial-State and Transition-State Solvent Effect on Reaction Rates and the Use of Thermodynamic Transfer Functions. *Acc. Chem. Res.* **1979**, *12*, 42–48.
100. Kramers, H. A. Brownian Motion in a Field of Force and the Diffusion Model of Chemical Reactions. *Physica* **1940**, *7*, 284–304.

101. Gavish, B.; Werber, M. M. Viscosity-Dependent Structural Fluctuations in Enzyme Catalysis. *Biochemistry* **1979**, *18*, 1269–1275.
102. Shaik, S. S. How Is Transition State Looseness Related to the Reaction Barrier? *J. Am. Chem. Soc.* **1988**, *110*, 1127–1131.
103. Westaway, K. C. Solvent Effects on the Structure of  $S_N2$  Transition States. *Can. J. Chem.* **1978**, *56*, 2691–2699.
104. Westaway, K. C.; Lai, Z.-G. Solvent Effects on  $S_N2$  Transition State Structure. II: The Effect of Ion Pairing on the Solvent Effect on Transition State Structure. *Can. J. Chem.* **1989**, *67*, 345–349.
105. Dashnau, J. L.; Nucci, N. V.; Sharp, K. A.; Vanderkooi, J. M. Hydrogen Bonding and the Cryoprotective Properties of Glycerol/Water Mixtures. *J. Phys. Chem. B* **2006**, *110*, 13670–13677.
106. Dudko, O. K.; Hummer, G.; Szabo, A. Intrinsic Rates and Activation Free Energies from Single-Molecule Pulling Experiments. *Phys. Rev. Lett.* **2006**, *96*, 108101.
107. Garcia-Manyes, S.; Liang, J.; Szoszkiewicz, R.; Kuo, T.-L.; Fernández, J. M. Force Activated Reactivity Switch in a Bimolecular Chemical Reaction. *Nat. Chem.* **2009**, *1*, 236–242.
108. Lide, D. R., Ed. *CRC Handbook of Chemistry and Physics*, 89th ed. (Internet Version 2009); CRC Press/Taylor and Francis: Boca Raton, FL, 2008; pp 9–78.
109. Beyer, M. K. Coupling of Mechanical and Chemical Energy: Proton Affinity as a Function of External Force. *Angew. Chem., Int. Ed.* **2003**, *42*, 4913–4915.
110. Marcus, R. A.; Sutin, N. Electron Transfers in Chemistry and Biology. *Biochim. Biophys. Acta* **1985**, *811*, 265–322.
111. Császár, P.; Csizmadia, I. G.; Viviani, W.; Loos, M.; Rivail, J. L.; Perczel, A. Breaking and Making of the S–S Linkage via Nucleophilic Substitution: An *Ab Initio* Study. *J. Mol. Struct. (THEOCHEM)* **1998**, *455*, 107–122.
112. Holmgren, A. Thioredoxin. *Annu. Rev. Biochem.* **1985**, *54*, 237–271.
113. Arnér, E. S. J.; Holmgren, A. Physiological Functions of Thioredoxin and Thioredoxin Reductase. *Eur. J. Biochem.* **2000**, *267*, 6102–6109.
114. Martin, J. L. Thioredoxin-a Fold for All Reasons. *Structure* **1995**, *3*, 245–250.
115. Wiita, A. P.; Perez-Jimenez, R.; Walther, K. A.; Gräter, F.; Berne, B. J.; Holmgren, A.; Sanchez-Ruiz, J. M.; Fernández, J. M. Probing the Chemistry of Thioredoxin Catalysis with Force. *Nature* **2007**, *450*, 124–127.
116. Szoszkiewicz, R.; Ainaravapu, S. R. K.; Wiita, A. P.; Perez-Jimenez, R.; Sanchez-Ruiz, J. M.; Fernández, J. M. Dwell Time Analysis of a Single-Molecule Mechanochemical Reaction. *Langmuir* **2008**, *24*, 1356–1364.
117. Holmgren, A. Reduction of Disulfides by Thioredoxin. Exceptional Reactivity of Insulin and Suggested Functions of Thioredoxin in Mechanism of Hormone Action. *J. Biol. Chem.* **1979**, *254*, 9113–9119.
118. Qin, J.; Clore, G. M.; Gronenborn, A. M. The High-Resolution Three-Dimensional Solution Structures of the Oxidized and Reduced States of Human Thioredoxin. *Structure* **1994**, *2*, 503–522.
119. Eklund, H.; Gleason, F. K.; Holmgren, A. Structural and Functional Relations among Thioredoxins of Different Species. *Proteins* **1991**, *11*, 13–28.
120. Qin, J.; Clore, G. M.; Kennedy, W. P.; Kuszewski, J.; Gronenborn, A. M. The Solution Structure of Human Thioredoxin Complexed with Its Target from Ref-1 Reveals Peptide Chain Reversal. *Structure* **1996**, *4*, 613–620.
121. Foloppe, N.; Nilsson, L. The Glutaredoxin -C-P-Y-C- Motif: Influence of Peripheral Residues. *Structure* **2004**, *12*, 289–300.
122. Xue, X. C.; Gong, L. C.; Liu, F.; Ouyang, Z. C. Two-Pathway Four-State Kinetic Model of Thioredoxin-Catalyzed Reduction of Single Forced Disulfide Bonds. *Phys. Rev. E* **2008**, *77*, 050903.
123. Perez-Jimenez, R.; Wiita, A. P.; Rodriguez-Larrea, D.; Kosuri, P.; Gavira, J. A.; Sanchez-Ruiz, J. M.; Fernández, J. M. Force-Clamp Spectroscopy Detects Residue Co-Evolution in Enzyme Catalysis. *J. Biol. Chem.* **2008**, *283*, 27121–27129.
124. Maier, B.; Koomey, M.; Sheetz, M. P. A Force-Dependent Switch Reverses Type IV Pilus Retraction. *Proc. Natl. Acad. Sci. U.S.A.* **2004**, *101*, 10961–10966.
125. Chen, S.; Springer, T. A. Selection Receptor-Ligand Bonds: Formation Limited by Shear Rate and Dissociation Governed by the Bell Model. *Proc. Natl. Acad. Sci. U.S.A.* **2001**, *98*, 950–955.
126. Kalluri, R. Basement Membranes: Structure, Assembly and Role in Tumour Angiogenesis. *Nat. Rev. Cancer* **2003**, *3*, 422–433.
127. Farina, A. R.; Tacconelli, A.; Cappabianca, L.; DeSantis, G.; Gulino, A.; Mackay, A. R. Thioredoxin Inhibits Microvascular Endothelial Capillary Tubule Formation. *Exp. Cell. Res.* **2003**, *291*, 474–483.
128. Grandi, F.; Sandal, M.; Guarguaglini, G.; Capriotti, E.; Casadio, R.; Samori, B. Hierarchical Mechanochemical Switches in Angiostatin. *ChemBioChem* **2006**, *7*, 1774–1782.
129. Sandal, M.; Grandi, F.; Samori, B. Single Molecule Force Spectroscopy Discovers Mechanochemical Switches in Biology: The Case of the Disulfide Bond. *Polymer* **2006**, *47*, 2571–2579.
130. Binnig, G.; Rohrer, H.; Gerber, C.; Weibel, E. Surface Studies by Scanning Tunneling Microscopy. *Phys. Rev. Lett.* **1982**, *49*, 57–61.
131. Weibel, E.; Binnig, G.; Quate, C. F.; Gerber, C. Atomic Force Microscope. *Phys. Rev. Lett.* **1986**, *56*, 930–933.
132. Moerner, W. E.; Kador, L. Optical Detection and Spectroscopy of Single Molecules in a Solid. *Phys. Rev. Lett.* **1989**, *62*, 2535–2538.
133. Orrit, M.; Bernard, J. Single Pentacene Molecules Detected by Fluorescence Excitation in a *p*-Terphenyl Crystal. *Phys. Rev. Lett.* **1990**, *65*, 2716–2719.
134. Ashkin, A.; Dziedzic, J. M.; Bjorkholm, J. E.; Chu, S. Observation of a Single-Beam Gradient Force Optical Trap for Dielectric Particles. *Opt. Lett.* **1986**, *11*, 288–290.
135. Ashkin, A.; Dziedzic, J. M. Optical Trapping and Manipulation of Viruses and Bacteria. *Science* **1987**, *235*, 1517–1520.
136. Amblard, F.; Maggs, A. C.; Yurke, B.; Pargellis, A. N.; Leibler, S. Subdiffusion and Anomalous Local Viscoelasticity in Actin Networks. *Phys. Rev. Lett.* **1996**, *77*, 4470–4473.
137. Kneipp, K.; Wang, Y.; Kneipp, H.; Perelman, L. T.; Itzkan, I.; Dasari, R.; Feld, M. S. Single Molecule Detection Using Surface-Enhanced Raman Scattering. *Phys. Rev. Lett.* **1997**, *78*, 1667–1670.
138. Nie, S. M.; Emery, S. R. Probing Single Molecules and Single Nanoparticles by Surface-Enhanced Raman Scattering. *Science* **1997**, *275*, 1102–1106.
139. Paravicini, T. M.; Touyz, R. M. Redox Signaling in Hypertension. *Cardiovasc. Res.* **2006**, *71*, 247–258.
140. World, C. J.; Yamawaki, H.; Berk, B. C. Thioredoxin in the Cardiovascular System. *J. Mol. Med.* **2006**, *84*, 997–1003.
141. Tao, L.; Gao, E.; Bryan, N. S.; Qu, Y.; Liu, H. R.; Hu, A.; Christopher, T. A.; Lopez, B. L.; Yodoi, J.; Koch, W. J.; Feelisch, M.; Ma, X. L. Cardioprotective Effects of Thioredoxin in Myocardial Ischemia and Reperfusion: Role of S-Nitrosation. *Proc. Natl. Acad. Sci. USA* **2004**, *101*, 11471–11476.
142. Thomas, W. E.; Vogel, V.; Sokurenko, E. Biophysics of Catch Bonds. *Annu. Rev. Biophys.* **2008**, *37*, 399–416.
143. Hummer, G.; Szabo, A. Free Energy Surfaces from Single-Molecule Force Spectroscopy. *Acc. Chem. Res.* **2005**, *38*, 504–513.
144. Dudko, O. K.; Hummer, G.; Szabo, A. Theory, Analysis, and Interpretation of Single-Molecule Force Spectroscopy Experiments. *Proc. Natl. Acad. Sci. U.S.A.* **2008**, *105*, 15755–15760.
145. Frank, I.; Aktah, D. Breaking Bonds by Mechanical Stress: When Do Electrons Decide for the Other Side? *J. Am. Chem. Soc.* **2002**, *124*, 3402–3406.
146. Johnson, C. P.; Tang, H. Y.; Carag, C.; Speicher, D. W.; Discher, D. E. Forced Unfolding of Proteins Within Cells. *Science* **2008**, *317*, 663–666.